University of Stavanger

Faculty of Science and Technology

MASTER'S THESIS

Study program/ Specialization: **Offshore Technology** **Marine- and Subsea Technology**	Spring semester, 2013 Open access
Author: **Ole-Erik Vestøl Endrerud**	…………………………………………… (Author's signature)
Faculty supervisor: **Ljiljana Djapic Oosterkamp, PhD** External supervisor: **Per Nystrøm, IKM Ocean Design**	
Title of thesis: **Parameter Study of the Effect of Boulders on Pipeline Free Span Sections**	
Credits (ECTS): **30**	
Key words: **Free spanning pipeline** **Vortex induced vibrations** **Boulder supports** **Pipeline dynamics** **Fatigue lifetime**	Pages: **64** + enclosure: **8** Stavanger, June 17th 2013 Date/year

ii

Acknowledgements

I'd like to thank everybody who helped me during the thesis work, and a special thanks to Statoil and IKM for sharing information, and having offices and software at my disposal. I also want to specially thank Dr. Ljiliana D. Oosterkamp (Statoil and UiS), Audun Schanche Kristoffersen (IKM), Zhengou Tu (IKM), Per Nystrøm (IKM) and Christer Eiken (fellow student) for all guidance, help and good discussions during my work.

Last but not least, I want to direct my love and gratefulness to my devoted and solicitous wife, Elisabeth, for all her support and care during this work.

Yours sincerely,

Ole-Erik Vestøl Endrerud

iv

Contents

List of Figures

List of Tables

Nomenclature

Abbreviations

CF	Cross-flow
DNV	Det Norske Veritas
FEA	Finite elemental analysis
ID	Internal steel diameter
IL	In-line
NCS	Norwegian Continental Shelf
OD	Outer steel diameter
ROV	Remotely Operated Vehicle
TD	Total diameter (OD incl. coating)
ULS	Ultimate limit state
VIV	Vortex induced vibrations

Greek Symbols

α	Thermal expansion coefficient
β	Flow velocity ratio
η	Dynamic viscosity
λ	Inverse of eigenvalue
μ	Friction coefficient
ν	Poissons ratio
ω	Natural frequency
ω^2	Eigenvalue
ρ_{cont}	Density of pipeline content
ρ_{corr}	Material density of corrosion coating

ρ_c	Material density of concrete coating
ρ_s	Material density of steel
σ_T	Steel tensile strength
σ_Y	Steel yield strength
θ_x	Rotation around x axis
θ_y	Rotation around y axis
θ_z	Rotation around z axis
ξ	Amplitude of oscillatory flow

Mathematical Symbols

σ_s	Mean effective stress of soils
$\triangle T$	Difference between installation temperature and operating temperature
A_e	Element cross section area
C	Constant for end conditions
C_D	Drag coefficient
$C_{L,max}$	Maximum lift force coefficient
C_M	Intertia coefficient
C_m	Hydrodynamic mass coefficient
D	Pipeline diameter
E	Young's modulus
e	Span gap $[m]$
e_s	Void ratio
f_{cn}	Construction strength of concrete coating
F_D	Drag force
$F_{friction}$	Friction force
F_I	Inertia force
f_n	Natural frequency
f_v	Shedding frequency
k	Stiffness
k_c	Concrete stiffness factor

K_L	Lateral dynamic soil stiffness
$K_{V,S}$	Vertical static soil stiffness
K_V	Vertical dynamic soil stiffness
k_w	Wave number
KC	Keuligan-Carpenter number
L	Free span section length
l_e	Element length
m	Free span section mass
m_a	Added mass
$m_{submerged}$	Submerged unit weight of the pipeline
OCR	Overconsolidation for cohesive soils
P	Effective axial force
P_E	Euler buckling load
P_i	Internal pressure
Re	Reynolds number
St	Strouhals number
t_{corr}	Corrosion coating thickness
t_c	Concrete coating thickness
t_s	Steel wall thickness
T_w	Wave period
U	Flow velocity
U_c	Current velocity
U_m	Maximum water particle velocity
U_w	wave velocity
u_x	Displacement in x direction
u_y	Displacement in y direction
u_z	Displacement in z direction
V_r	Reduced velocity
z	Virtual anchor distance

Chapter 1

Introduction

1.1 Background

Hydrocarbons are the most important energy resource in the world today, especially oil and more recently gas. Energy is one of the driving forces for development of societies and economies, and is besides food and clean water the most important resource for human kind; nevertheless, this resource becomes scarcer every year.

Export of gas from the Norwegian Continental Shelf (NCS) to Europe is facilitated thorough a comprehensive network of 10.000 kilometres of export pipelines, operated by Gassco and maintained by various service providers – Statoil being the largest.

Excellent pipeline integrity management is crucial to avoid devastating environmental disasters, lethal accidents, and massive economical losses. Free spanning pipelines are one threat to pipeline integrity. Damages caused by free spanning pipelines are buckling, over-stressing from sagging, and fatigue damage. Buckling and sagging can be visually identified, as opposed to fatigue. The concern for fatigue is because of its anonymity, low probability of discovery, and high consequences of failure.

1.2 Literature Review

Free spanning pipelines is a common industrial issue, and dynamic behaviour of pipelines has been investigated by the academic community for decades. This literature review is meant to determine the level of academic and industrial interest in long free spans and what other important studies have been conduced on the topic of long free spans, especially other parameter studies of the phenomena. The methodology used for this survey is to search common databases (e.g. SpringerLink, EBSCO, ScienceDirect, and Scopus) with predetermined search queries.

The accepted approach for free span assessments is according to DNV-RP-F105, which applies a semi-empirical response model approach to predict vibration amplitudes caused by vortex shedding [17]. In case of very complex spans or exceedance of the limitations of this method a finite elemental analysis (FEA) need to be applied to analyse natural modes and frequencies. Generally, a FEA analysis is less preferred because of resource consummation, and where possible and reasonable the semi-empirical method is applied.

FEA is a numerical method used for accurate solutions of complex mechanical and structural systems, e.g. solve eigenvalue problems of such systems. The FE method replaces a mechanical or structural system with elements, which are assumed to behave as a continuous structural member – a finite element [12]. Because finding an exact solution is very difficult for complex systems, an approximate solution is found for each element. One then selects an appropriate solution for each element, which will then converge to the exact solution for very small element sizes.

Recently a semi-analytical approach was developed by Sollum and Vedeld [14], which, is very accurate compared with the FEA method, even for long free spans, and requires a considerably lower level of resources compared to FEA.

There are several influencing parameters to consider in relation to vortex induced vibrations. A pipeline in close proximity of the sea bottom, as a free span could be, will experience a wall effect as a function of gap ratio (e/D).

Mutlu-Sumer and Fredsøe [16] prepared a review of research done on the area, and indicate that vortex shedding will be suppressed by placing pipelines close to the seabed. For gap-to-diameter ratios down to 0.3, there is no noticeable effect. However, for gap ratios below 0.3, vortex-shedding suppression will increase as gap ratios decrease. The reason for this is the asymmetric generation of vortices between the two sides of the pipeline. Vortices created at the upper side will be larger and stronger thus hinder interaction between the two vortices [16].

Wall proximity has a suppressive effect for oscillatory flow as well[16]. For large values of KC ($< 40 - 50$), the boundary where vortex shedding is suppressed approaches the same gap ratio as for constant current. For smaller values of KC, the suppression boundary decreases for decreasing KC. Meaning the vortex shedding is maintained for smaller gap ratios, hence the wall proximity has a lower effect.

Another wall effect could be an increased drag term from increased added mass. When a small gap traps a volume of fluid between the pipeline and seabed, the friction (viscous) forces could hinder this volume of fluid from escaping. Hence, this volume of fluid will extend the pipeline geometry to the seabed and act as an "invisible" wall.

Fyrilev and Collberg [8] provides an extensive explanation of the concept

of effective axial force and the effect of internal pressure on natural frequency of pipelines. In their paper they deduce that the effect of increasing internal pressure will decrease the natural frequency of a span, and, thus, increase the risk of VIV and fatigue failure.

In relation to the influence of effective axial force, Søreide et al. [15] investigates the effect of sag on the natural frequency of free spans. Their conclusion from analysing sag effects is that sagging will increase the natural frequency of symmetric cross flow (CF) modes (1. mode, 3. mode, 5. mode, etc.) while anti-symmetric modes and in-line (IL) modes are left unaffected.

Span corrections in terms of introducing boulders to move the natural frequencies of a span away from the vortex shedding frequency is the conventional approach, see e.g. [15]. However, the location of such boulders is suspected to be inefficient if located at null-points of vibration modes, and especially dangerous if it is the second or third mode. As a rule of thumb in the industry, locating boulders at these null-points will not have an effect, and one can assume a dynamic behaviour of two neighbouring spans with a small boulder between act as a span with the combined length of the two at these modes. In addition, the contact length of boulders will have an effect on span dynamics, in governing if spans are interacting or not.

For a non-FEA approach Det Norske Veritas (DNV) recommends in DNV-RP-F105 [17] to screen if a span interacts or not by comparing neighbouring span lengths with shoulder length, while Statoil has set a criteria that spans with shoulders exceeding six meters are not interacting. If an FEA approach is used one can identify depending on a modal analysis wether or not spans are interacting.

1.3 Problem Description

Free spanning pipelines are one threat to pipeline integrity. Damages caused by free spans are buckling, over-stressing due to sagging, and fatigue damage due to vortex induced vibrations (VIV) and direct wave loads.

The current working practice when surveying offshore pipelines is to report on specific elements and items along the pipeline; for example free spans, boulders, alien objects, etc. For free spans the current requirement is to report on shoulder supports that are larger than one total diameter (TD). As a consequence one has seen a number of extremely long free spans, which almost defies the laws of physic. The reason are shoulder supports that are less than one TD not being reported.

Looking back to the issue of fatigue, pipeline dynamics are of outmost importance. Introducing a boulder resulting in two adjacent free spans in stead of one long can change the dynamic response of a pipeline. Hence, one must investigate how introducing small supports to free spans alters the dynamic response, and, in the end fatigue lifetime.

1.4   Research Questions

- Is a multi span with boulders located at vibrational null-points equivalent to a single span with a length equal to all multi spans combined?

- How will contact length of boulders influence the dynamic behaviour of a multi span?

1.5   Limitations

In this study the focus will be on vortex induced vibrations caused by constant flow, i.e. currents, hence, VIV due to waves and direct wave loading will not be subject to investigation in the analysis. Although, wave forces and VIV due to waves have been included for completeness in Chapter 2.

Chapter 2

Theory

One can look at a free spanning pipeline as a guitar string. It moves as a mechanical wave, and have modes of vibration. Depending on the pretension of the guitar string, different tones appear; i.e. different vibrational frequencies and amplitudes. Pretension in the case of subsea pipelines can result from residual lay tension, internal and external pressures, thermal expansion and sagging. Your finger is the force acting on the guitar string to make it vibrate just like waves and currents will force a free spanning pipeline to vibrate. These vibrations can cause failure due to fatigue of a free spanning pipeline, due to the number of cycles combined with dynamic stress resulting from vibration amplitudes.

This chapter introduces a portion of the vast material on vortex induced vibrations, in general and for pipelines, and fatigue theory as a reference for the reader.

2.1   Vortex Induced Vibrations – VIV

A cylinder submerged in water will experience a fluid flow (which is the analogue to a pipeline free span section) due to waves and currents. Because of forces from this fluid flow, the pipeline can experience vibrations due to vortex shedding, designated as vortex-induced vibrations. This phenomenon will be explained shortly in the preceding part. Two separate cases are of interest when examining VIV on offshore pipelines; constant current and oscillatory flow (waves). If linearised wave theory (Airy) is assumed, wave effects can easily be neglected in deep waters, and constant current can be assumed. In this study deep water will be assumed, furthermore, VIV due to waves and direct wave loading will not be considered.

2.1.1   Important Parameters

Reynolds Number (Re)

Flow regimes are characterised by the Reynolds number

$$Re = \frac{DU}{\eta} \tag{2.1}$$

where D is the pipeline diameter, U is the flow velocity, and η is the dynamic viscosity. Reynolds number is a ratio between the inertia and the viscous (frictional) force in a flow. Very low Reynolds numbers indicate laminar steady flow, while a high Reynolds number indicate unsteady turbulent flow.

Strouhals Number (St)

The normalised shedding frequency is called the Strouhals number

$$St = \frac{f_v D}{U} \tag{2.2}$$

where f_v is the shedding frequency. For cylindrical shaped bodies – like pipelines – the Strouhal number remains fairly constant from $300\,Re$ to the end of the subcritical flow regime at $3 \times 10^5\,Re$ [16]. It is in this region the power spectra is at its highest, with a distinct peak at $0.2\,St$ [13].

Keulegan-Carpenter Number (KC)

The Keuligan-Carpenter number is defined as

$$KC = \frac{U_m T_w}{D} \tag{2.3}$$

where U_m is the maximum water particle velocity, and T_w is the wave period. KC can alternatively be expressed as [16]

$$KC = \frac{2\pi\xi}{D} \tag{2.4}$$

here expressed with the amplitude of oscillatory flow ξ. As the Reynolds number represents flow in constant current, the Keulegan-Carpenter number represents oscillatory flow of water particles.

Reduced Velocity (V_r)

Another non-dimensional parameter that is important with respect to vortex-induced vibrations is the reduced velocity, V_r, which is the normalised flow velocity. V_r is represented by

$$V_r = \frac{U}{f_n D} \tag{2.5}$$

where f_n is the natural frequency of the pipeline, expressed by [4]

$$f_n = \frac{C}{L^2} \sqrt{\frac{EI}{(m + m_a)}} \sqrt{1 - \frac{P}{P_E}} \tag{2.6}$$

where C is a constant for end conditions, L is free span section length,E is Young's modulus, m is the free span section mass, m_a is added mass, P is the effective axial force (residual lay tension, forces from bending and sag, thermal expansion, external pressure and internal pressure), P_E is the Euler buckling load.

2.1.2 Vortex Shedding

Boundary Layer

Real fluids are viscous. Consequently, fluids experience friction forces when passing a submerged cylinder, creating what is called the boundary layer. The boundary layer is a layer of fluid close to the cylinder body, where viscous (friction) forces dominates and decelerate the surrounding water particle flow.

A boundary layer exists because of the no-slip condition, which means that particles of fluid adhere to the submerged body so its velocities reduces to zero at the cylinder body surface [7].

This implies there will exist an adverse pressure gradient, which means the pressure is increasing in the direction of the flow and the potential energy increases. This is due to the water particle velocity close to the boundary layer being slowed down (it can be proven by Bernoulli´s equation).

Flow velocity increases with distance from the cylinder surface. Because shear forces between the fluid layers are not zero, the larger flow velocity outside the boundary layer will introduce rotation in the flow; vortices.

When the water particle velocity close to the boundary layer reaches zero it reverts (because flow wants to go from high to low pressure), and the water particles are forced of the boundary layer. The effect of boundary layer separation is vortex formation.

A boundary layer will have three stages of flow (ref. Figure 2.1): laminar, transitional, and turbulent. In the transcritical flow regime the boundary layers are completely turbulent, while in the subcritical flow regime the boundary layers are laminar (ref. Figure 2.2).

Vortex Shedding in Constant Current

Figure 2.2 illustrates different flow regimes around a pipeline for different Re. For Re lower than five there is no boundary layer separation and flow
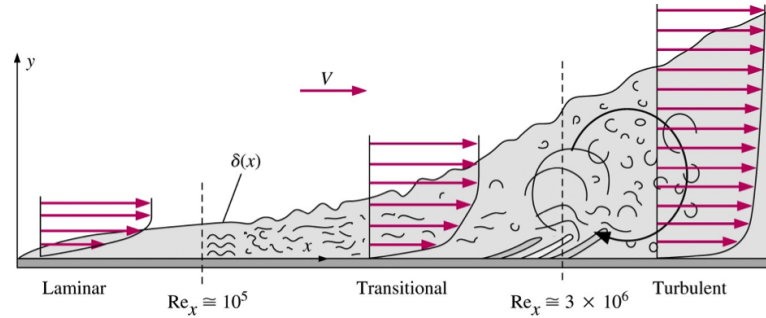
Figure 2.1: Boundary layer separation [11]

is steady and laminar.

Boundary layer starts to separate and vortices start to appear between 5 and 40 Re as standing symmetric vortices in the wake. At Re between 40 and 200 the wake becomes unstable and vortices shed from the wake, forming a laminar vortex street [16]. This is the phenomenon of vortex shedding.

First, vortices shed simultaneously, then with increasing flow velocity the vortex shedding starts alternating. When Reynolds number pass 300, formed vortices are completely turbulent and are noticeably three-dimensional [19]. Pressure on the upper surface and lower surface will decrease and increase periodically, resulting in an oscillating lift force. Thus, the circular body will vibrate normal to the flow direction.

As said previously, the Strouhals number remains fairly constant 0.2 for a pipeline, from 300 Re to the end of the subcritical flow regime at $3 \times 10^5 \, Re$ [16]. It is in this Reynolds number region the power spectra is at its highest, with a distinct peak at $0.2 \, St$ [13]. When the flow goes from subcritical to supercritical the Strouhal number makes a jump to 0.7, and the pipeline vibration amplitude decrease noticeably.

Vortex Shedding in Oscillatory Flow

When describing oscillatory flow, e.g. in a wave situation, the Keuligan-Carpenter number is commonly used. Low KC indicates that the orbital motions[1] of water particles are of such a small magnitude separation of the boundary layer might not occur. Large KC indicates from equation 2.4 that the oscillatory flow amplitude, hence distance travelled by water particles, is large compared to the pipeline diameter and vortex shedding might occur. For very large KC the flow can be considered as a constant current [2]. Flow

---

[1]Water particles have an elliptic orbital motion, which mathematically can be represented by a trajectory with x and z components: $(x - x_0)^2 + (z - z_0)^2 = \left(\xi \cdot e^{k_w z_0}\right)^2$ for deep water. For a more thorough analysis of water particle motions see [9].
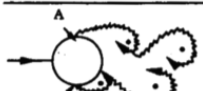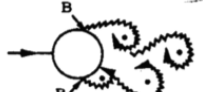
a)		No separation. Creeping flow	Re < 5
b)		A fixed pair of symmetric vortices	5 < Re < 40
c)		Laminar vortex street	40 < Re < 200
d)		Transition to turbulence in the wake	200 < Re < 300
e)		Wake completely turbulent. A:Laminar boundary layer separation	$300 < Re < 3 \times 10^5$ Subcritical
f)		A:Laminar boundary layer separation B:Turbulent boundary layer separation;but boundary layer laminar	$3 \times 10^5 < Re < 3.5 \times 10^5$ Critical (Lower transition)
g)		B: Turbulent boundary layer separation;the boundary layer partly laminar partly turbulent	$3.5 \times 10^5 < Re < 1.5 \times 10^6$ Supercritical
h)		C: Boundary layer completely turbulent at one side	$1.5 \times 10^6 < Re < 4 \times 10^6$ Upper transition
i)		C: Boundary layer completely turbulent at two sides	$4 \times 10^6 < Re$ Transcritical

Figure 2.2: Flow regimes around a pipeline in constant current [16]

regimes for increasing KC are illustrated in Figure 2.3. From the figure vortex shedding occurs for $KC > 7$.

2.1.3   Forces on a Submerged Cylinder

There are two main forces acting on a submerged pipeline; namely drag, and lift. The drag force acts in-line with the flow, and the lift force acts perpendicular to the flow. Forces from current and waves are different. Forces from water particle movement due to current come from a constant flow, while, on the other hand, forces due to waves come from an oscillating flow.

Forces in Constant Current

Drag force consists of pressure drag and friction drag. However, in the subcritical flow regime (*Re* between 300 and 3×10^5) contribution from friction drag is in the order of 2-3 % [16], and can be neglected.

Pressure drag is far more important. This force is present because flow velocity is lower in the wake behind the pipeline than outside the wake. This, according to Bernoulli, creates a pressure pushing the pipeline against the flow, as seen in Figure 2.4. However, this pressure is usually lower than the pressure exerted at the stagnation point at the pipeline front. Consequently, a net pressure drag force exists in the flow direction. Pressure drag will vary with time when vortex shedding occurs. Furthermore, the drag force will have a frequency twice the shedding frequency, because during every vortex shedding the pressure drag will complete one full cycle. However, the amplitude for in-line vibrations is considerably lower than the cross-flow vibrations.

An alternating cross-flow lift force, will occur when Re is larger than 40 when vortex shedding appears. This is because of the fluctuating pressure distribution with respect to time due to vortex shedding, seen in Figure 2.4. From this figure, one can see that the downward lift force is due to creation of the upper vortex, and the upward lift force due to creation of the lower vortex. Moreover, the fluctuating pressure occurs as a consequence of lowered fluid flow velocity, which leads to increasing pressure. Cross-flow vibrations are due to this fluctuating lift force, and will have the same frequency as the shedding frequency. Cross-flow vibration amplitudes can get high depending on flow velocity.

Forces in Oscillatory Flow

As for constant current, there exist a lift and drag force in oscillatory flow. In addition to the drag force, there exist a hydrodynamic mass force (added mass) and the Froude-Krylov force.
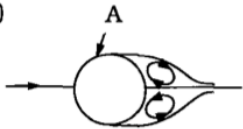
a)	No separation. Creeping (laminar) flow.	KC < 1.1
b)	Separation with Honji vortices. See Figs. 3.3 and 3.4	1.1 < KC < 1.6
c)	A pair of symmetric vortices	1.6 < KC < 2.1
d) A	A pair of symmetric vortices. Turbulence over the cylinder surface (A).	2.1 < KC < 4
e)	A pair of asymmetric vortices	4 < KC < 7
f)	Vortex shedding	7 < KC Shedding regimes

Figure 2.3: Flow regimes around a pipeline in oscillatory flow (waves) [16]
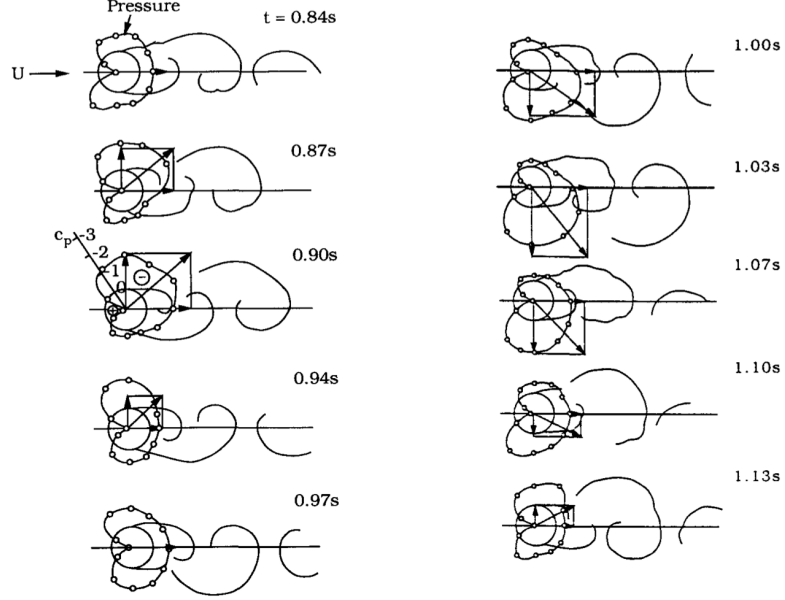
Figure 2.4: Pressure distribution on a pipeline in constant current [16]

The total in-line force is described by Morison's equation [10]

$$F_{IL} = \frac{1}{2}\rho C_D DU \left| U \right| + \rho C_M A \dot{U} + \rho A \dot{U} \qquad (2.7)$$

where C_D is the drag coefficient, and C_m is the hydrodynamic mass coefficient ($C_m = 1$ for smooth cylinders and low KC [16]). Equation 2.7 can alternatively be written in a more familiar form

$$F_{IL} = \frac{1}{2}\rho C_D DU \left| U \right| + \rho C_M A \dot{U} \qquad (2.8)$$

where the first expression is the drag force and second expression is the inertia force

$$F_D = \frac{1}{2}\rho C_D DU \left| U \right| \qquad (2.9)$$

$$F_I = \rho C_M A \dot{U} \qquad (2.10)$$

where C_M is the inertia coefficient

$$C_M = 1 + C_m \qquad (2.11)$$

In linear wave theory where the displacement is harmonic the two time derivatives velocity and acceleration are 90° out of phase with each other. Hence, the maximum of drag force and inertia force will not occur at the same time. The ratio between these two forces can be derived for low KC

$$\frac{F_I}{F_D} = \frac{C_M \frac{\pi}{4} D^2 \omega U_m}{\frac{1}{2} C_D D U_m^2} = \pi^2 \frac{D}{U_m T_w} \frac{C_M}{C_D} = \frac{\pi^2}{KC} \frac{C_M}{C_D} \qquad (2.12)$$

And with appropriate values for C_M and C_D for circular cylinders the ratio becomes

$$\frac{F_{I,max}}{F_{D,max}} = \frac{\pi^2}{KC} \frac{2}{1} \approx \frac{20}{KC} \qquad (2.13)$$

From equation 2.13, it is clear that for low KC the inertia force is dominating. The lift force will be equal to zero for $KC < 4$ due to zero vortex shedding. However, when $KC > 4$ vortices start to appear, and after $KC > 7$ there exist a lift force regime. This lift force will oscillate at a natural frequency different from the wave natural frequency, and will be depending on KC [16]. The number of oscillations will increase with increasing KC. The maximum lift force can be calculated according to

$$F_{L,max} = \frac{1}{2} \rho C_{L,max} D U_m^2 \qquad (2.14)$$

where $C_{L,max}$ is the maximum lift force coefficient. Experimental data show that $C_{L,max}$ reaches a maximum for $KC = 10$ and $Vr = 6$.

2.1.4 Vibrations of a Submerged Cylinder

As said before this study is concerned with VIV due to currents, hence, vortex shedding induces vibrations in the pipeline. There has been a discussion in the preceding section about the forces causing vibrations due to vortex shedding. The purpose of this section is to explain the very familiar calculation of natural frequencies of beams according to FEA and mechanical vibration theory, in addition to a short explanation of vibration modes in relation to in line and cross flow vibrations of free spanning sections of pipelines.

Natural Frequencies of an Euler-Bernoulli Beam

Any mechanical system given an initial energy, in the form of displacement or force, have a natural frequency, such that if no dissipation of energy occurred it would vibrate infinitely. All mechanical systems experience energy dissipation in the form of damping, and pipelines experience damping due to e.g. the soil it is situated on and the surrounding water. However, at this natural frequency (or frequencies as will be explained in the modes section)

energy is transferred into the system at a high rate, hence, large vibration amplitudes occur.

To determine the natural frequency of a pipeline's free span section one have to solve an eigenvalue problem, expressed as

$$(\lambda [k] - [m]) \vec{W} = \vec{0} \tag{2.15}$$

where k is the stiffness, $[k]$ is the stiffness matrix, $[m]$ is the mass matrix and

$$\lambda = \frac{1}{\omega^2} \tag{2.16}$$

is the inverse of the eigenvalue ω^2, the vector

$$\vec{W} = \left\{ \begin{array}{c} W_1 \\ W_2 \\ W_3 \\ \vdots \\ W_n \end{array} \right\} \tag{2.17}$$

is the mode shape or displacement of the system and the vector

$$\vec{0} = \left\{ \begin{array}{c} 0 \\ 0 \\ 0 \\ \vdots \\ 0 \end{array} \right\} \tag{2.18}$$

is the null vector. Here ω represents f_n the natural frequency of the system. Alternatively written

$$(\lambda [I] - [D]) \vec{W} = \vec{0} \tag{2.19}$$

where $[I]$ is the identity matrix and

$$[D] = [k]^{-1} [m] \tag{2.20}$$

According to equation 2.15, the trivial solution to this problem is that $\vec{W}$ is zero, but this does not give a satisfactory solution. For a non-trivial solution the determinant

$$|\lambda [k] - [m]| = 0 \tag{2.21}$$

must be zero.

This determinant will now be solved by the finite element method for an Euler-Bernoulli beam. As said before the FE method replaces a mechanical or structural system with elements, which are assumed to behave as a
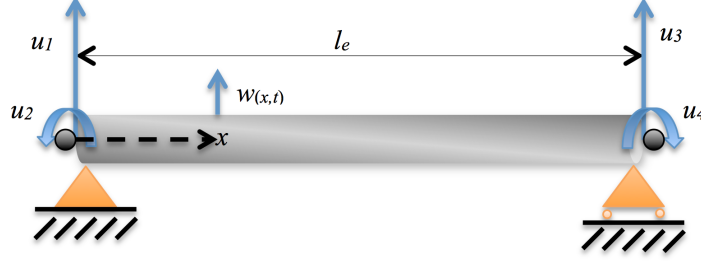
Figure 2.5: Euler-Bernoulli beam element

continuous structural member. In the FE method each elements end point is a node, which, in a three dimensional system has at least six degrees of freedom (u_x, u_y, u_z, θ_x, θ_y, θ_z). Each degree of freedom represents a row and column in the stiffness and mass matrixes. These nodes are connecting the elements together.

For simplicity, since this is just an explanation, only one element is used to model a section of free spanning pipeline and only cross flow vibrations are considered. With only one element the local coordinate system is equal to the global.

First, the global stiffness and mass matrixes must be determined, which is done by determining the expressions for kinetic and strain (potential) energy, see e.g. [12]. For a free span section modelled as an Euler-Bernoulli beam (shown in Fig. 2.5) with simply supported ends, element length l_e and element cross section area A_e they are

$$[K] = \frac{EI}{l_e^3} \begin{bmatrix} 12 & 6l_e & -12 & 6l_e \\ 6l_e & 4l_e^2 & -6l_e & 2l_e^2 \\ -12 & -6l_e & 12 & -6l_e^2 \\ 6l_e & 2l_e^2 & -6l_e^2 & 4l_e^2 \end{bmatrix} \tag{2.22}$$

$$[M] = \frac{\rho A l_e}{420} \begin{bmatrix} 156 & 22l_e & 54 & -13l_e \\ 22l_e & 4l_e^2 & 13l_e & -3l_e^2 \\ 54 & 13l_e & 156 & -22l_e \\ -13l_e & -3l_e^2 & -22l_e & 4l_e^2 \end{bmatrix} \tag{2.23}$$

Due to the fact that the local and global coordinate system is equal in this simple case $u_1 = W_1$, $u_2 = W_2$ and so on. Because of the simply supported boundary conditions at each end of the free span section $W_1 = 0$ and $W_3 = 0$, hence row 1 and 3 in addition to column 1 and 3 are deleted accordingly. One is then left with the following stiffness and mass matrixes

$$[K] = \frac{2EI}{l_e} \begin{bmatrix} 2 & 1 \\ 1 & 2 \end{bmatrix} \tag{2.24}$$

$$[M] = \frac{\rho A l_e^3}{420} \begin{bmatrix} 4 & -3 \\ -3 & 4 \end{bmatrix} \tag{2.25}$$

and the determinant in equation 2.21 can be written as

$$\left| \frac{2EI}{l_e} \begin{bmatrix} 2 & 1 \\ 1 & 2 \end{bmatrix} - \frac{\rho A l_e^3 \omega^2}{420} \begin{bmatrix} 4 & -3 \\ -3 & 4 \end{bmatrix} \right| = 0 \tag{2.26}$$

and by multiplying through by $l_e/2EI$ one gets

$$\begin{vmatrix} 2 - 4\lambda & 1 + 3\lambda \\ 1 + 3\lambda & 2 - 4\lambda \end{vmatrix} = 0 \tag{2.27}$$

where

$$\lambda = \frac{\rho A l_e^4 \omega^2}{840 EI} \tag{2.28}$$

Solving equation 2.27 the eigen value equation is obtained

$$\begin{vmatrix} 2 - 4\lambda & 1 + 3\lambda \\ 1 + 3\lambda & 2 - 4\lambda \end{vmatrix} = (2 - 4\lambda)^2 - (1 + 3\lambda)^2 = 3 - 22\lambda + 7\lambda^2 \tag{2.29}$$

The roots of this equation yield the natural frequencies for the beam system

$$\lambda_1 = \frac{1}{7} \Rightarrow \omega_1 = \sqrt{\frac{120 EI}{\rho A l_e^4}} \tag{2.30}$$

$$\lambda_2 = 3 \Rightarrow \omega_2 = \sqrt{\frac{2520 EI}{\rho A l_e^4}} \tag{2.31}$$

Increasing the number of elements will increase the accuracy of the numerical analysis of natural frequencies.

Modes and Mode Shapes

For each natural frequency $f_{n,i}$ (or ω_i) there exist a corresponding mode shape vector $\vec{W}$ which represents the movement and amplitudes of the pipeline. The modes can be idealised to look like different sinusoidal, where each mode number indicates an additional half sine wave. Furthermore, each even mode is a symmetric mode, while each odd mode is asymmetric, as illustrated in Figure 2.6.

Higher modes will on the same pipeline length have an increasing number of curves resulting in a higher local stress. However, the amplitudes in these higher modes are normally not very large compared to the first mode. The pipeline will not only vibrate two-dimensionally like shown above, but
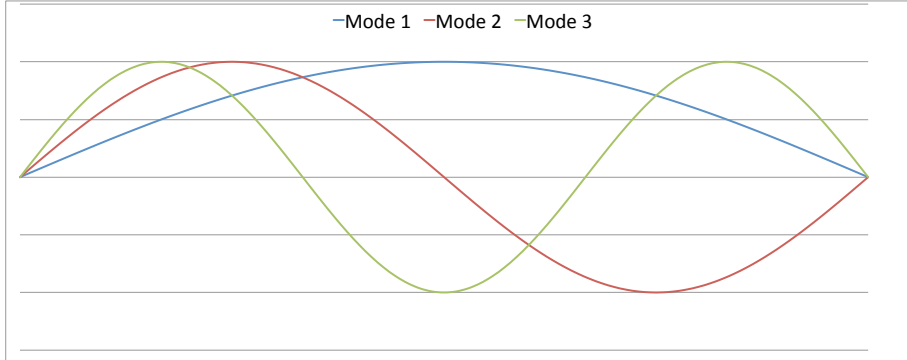
Figure 2.6: Mode shapes of the first three modes for a pipeline

three-dimensional, both in line with the flow and perpendicular to the flow (IL and CF vibrations).

As these vibrations result from vortex shedding modes will only be active if shedding occurs. When a pipeline free span section will experience vortex shedding can be determined from the reduced velocity (ref. section 2.1.1). As an example, for a 42" pipeline with a 100 meter span ($L/D = 93.8$) vibrations will occur for the first mode IL and CF when

$$V_{r,IL} = 3 \implies U = V_r f_{n,1,IL} D = 3 \cdot 0.287\,Hz \cdot 1.066\,m = 0.918\,m/s \quad (2.32)$$

$$V_{R,CF} = 8 \implies U = V_r f_{n,1,CF} D = 8 \cdot 0.409\,Hz \cdot 1.066\,m = 3.488\,m/s \quad (2.33)$$

Hence, it is not very likely that cross flow vibrations will occur under normal conditions for this span. Moreover, if one examines the equations, a longer free span will have a lower natural frequency, hence, a lower flow velocity is required for the shedding frequency to lock-in on the natural frequency of the pipeline free span section.

Normally the first mode is activated before the second one, and so on. But in some instances a higher mode can be activated before a lower one, for example because of extensive sagging (see e.g. [15]).

As seen in the example (equation 2.32 and 2.33) it is normally only the lower modes, the first three or four, that are activated by vortex shedding.

Soil Damping

The pipeline, which is situated on a flexible seabed, will experience modal damping depending on the stiffness of the seabed soil. One distinguish between cohesive and cohesion-less soils, or clays and sand, respectively.

This soil damping results from Coulomb friction and soil penetration when pipelines vibrate and during installation.

In an FEA modal analysis pipeline-soil interaction is modelled as Coulomb friction determining the dynamic soil stiffness, which contributes to the system stiffness matrix. Dynamic soil stiffness can be calculated for lateral (K_L) and vertical (K_V) directions according to DNV-RP-F105

$$K_V = \frac{0.88 \cdot G}{1 - \nu} \tag{2.34}$$

$$K_L = 0.76 \cdot G \cdot (1 + \nu) \tag{2.35}$$

where ν (Poisson's ratio) typically equals 0.45 for cohesive soils and 0.35 for cohesion-less soils, and the soil shear strength

$$G = 625 \cdot \frac{OCR^{k_s}}{0.3 + 0.7e_s^2} \sqrt{101 \cdot \sigma_s} \tag{2.36}$$

where OCR is the over-consolidation for cohesive soils (taken as 1 for cohesion-less soils), k_s is a coefficient taken from DNV-RP-F105 Figure D2, e_s is the void ratio (typically between 0.3 and 3 for cohesive soil and 0.4 and 0.9 for cohesion-less soils) and σ_s the mean effective stress of soils.

Accurate calculation of soil damping is a very tedious and complicated task, and requires a full geotechnical investigation of the specific locations of interest. As a consequence one can find typical values for different soil types in DNV-RP-F105. For a detailed description of determining soil damping see [17].

2.2   Fatigue Theory

Fatigue is failure of a structural member due to repeated number of load cycles at a stress amplitude below the yield and tensile strength of the material. Several factors affect the fatigue life, such as stress concentration, corrosion, range of stress and material properties (see e.g. [5], [6]). Cyclic loading on pipeline free spans come from VIV, direct wave loading or trawl impacts and stress concentration occurs at field joints between the concrete layer and steel cylinder.

Remaining life of the pipeline section subject to free spanning is calculated by applying S-N curves and the Palmgren-Miner damage accumulation rule. Both these methods are explained below. Another more advanced and complex method of determining fatigue life is to apply fracture mechanics.

2.2.1   S-N Curves

Fatigue capacity of materials are difficult to attain analytically, but based on experimental results a material's fatigue capacity at different stress am-
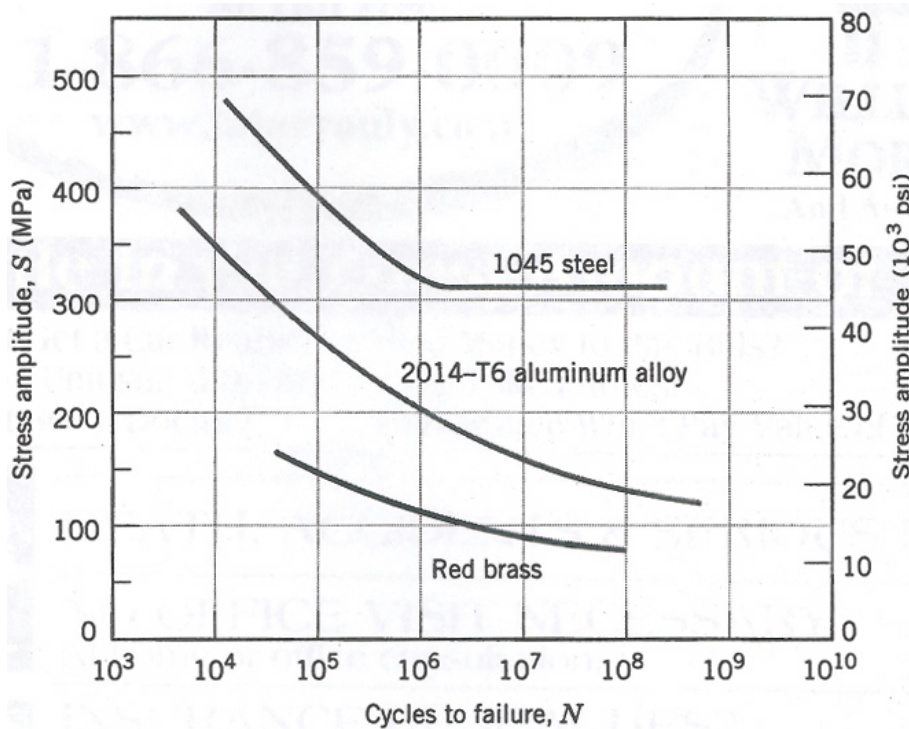
Figure 2.7: Example of S-N curves for different materials

plitudes is plottet to form an S-N curve. S represents stress amplitude and N the number of cycles at that stress amplitude causing a failure. Experiments to determine the S-N curve involves applying cyclic loading at a fixed stress cycle to an idealised rod of the specific material until it fails. An example of S-N curves for different metals is shown in Figure 2.7. Also important to mention is that some materials exerts an endurance limit, a stress amplitude at which the fatigue life (number of cycles) is infinite.

As an example, a structural member of 1045 Steel can experience approximately 10^5 number of cycles at $400\,MPa$ before failing (see Figure 2.7). In the same example, if the stress amplitudes never exceed $300\,MPa$ the member will never fail, because it is below the endurance limit.

2.2.2 Palmgren-Miner Damage Accumulation Rule

In 1924 Palmgren proposed a rule to calculate when a fatigue failure will occur based in accumulation of fatigue damage from each stress cycle a structural member experiences. This rule was popularised by Miner in 1945; hence the Palmgren-Miner damage accumulation rule.
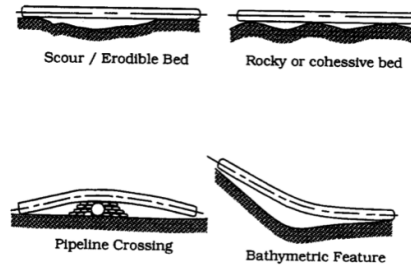
Figure 2.8: Formation of free spans [16]

The idea is that a structural member will fail when

$$D = \sum \frac{n_i}{N_i} = 1 \tag{2.37}$$

where n_i is the experienced number of cycles at the i-th stress cycle (σ_i) and N_i is the number of cycles at σ_i at which a failure will occur. Experimental data have shown that a failure occur for D between 0.7 and 2.2, but is normally taken as 1.

When assessing the fatigue life of a pipeline free span section the cumulative damage from current and wave VIV is calculated for all current and wave directions, each with a probability of occurrence. For more details on the conventional approach for fatigue life calculations see [17].

2.3   Description of Free Spans

2.3.1   Formation of Free Spans

Free spans can be designed in because of the morphology of the seabed, or be created due to dynamics of the seabed. Examples of free spans and seabed morphology are shown in Figure 2.8.

The seabed can have a rocky surface with peaks and foundations for free spans, these are often accounted for in design, but the pipeline can move substantially during its life cycle.

Sand dunes can also be present at the seabed and can act as free span foundations, if the radius of curvature is smaller than the radius of curvature of the pipeline. Sand foundations have the ability to be moved by current and waves. Furthermore, this can develop into subsea sand waves that develop free spans quickly, and an area that looked fine and no free spans were present can rapidly be altered by a moving sand wave and create free spans.

In addition, scouring is a threat when sand is the supporting soil. As illustrated in Figure 2.9, scouring is the process of washing out the soil
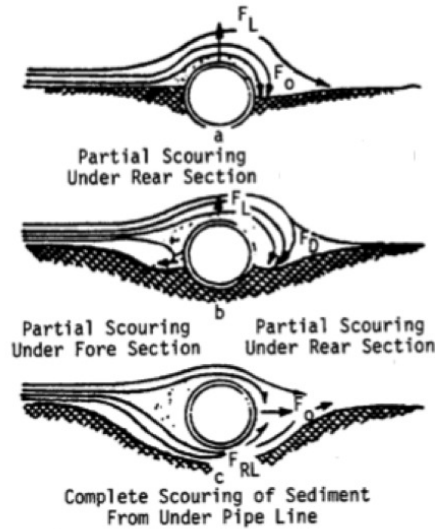
Figure 2.9: Formation of free spans by scouring

beneath the pipeline – hence, creating a free span.

On the Norwegian Continental Shelf there have been laid a large amount of pipelines, hence, pipeline crossings will exist and be a source of free spans. These possible free spans scenarios can be accounted for in design when the pipeline is designed and planned, by analysing surveys of the seabed.

The risk of forming free spans can be mitigated by different measures. Dredging and burying of pipelines is expensive but effective, and can eliminate the problem. However, this will limit the access to the pipeline for monitoring of the pipeline exterior, and can be excavated by scouring and moving sand. Another possibility is to rock dump beneath the pipeline to create fixed support. In this sense, this can create a situation where a new free span can form with a fixed support in one end.

Both these processes of burying and rock dumping are expensive and require vessel and ROV intervention, transport of rock, etc.

2.3.2 Classification of Free Spans

Pipeline free spans are classified according to certain criteria. Different practices exist, although Det Norske Veritas has developed a standard classification. In addition, companies develop company specific classifications.

First, because of the importance of dynamics, free spans have to be classified as interacting or isolated free spans. If a free span is interacting with a neighbouring span, it can have a complex dynamic behaviour especially if it experiences multi-mode vibrations. Whether a free span is interacting or
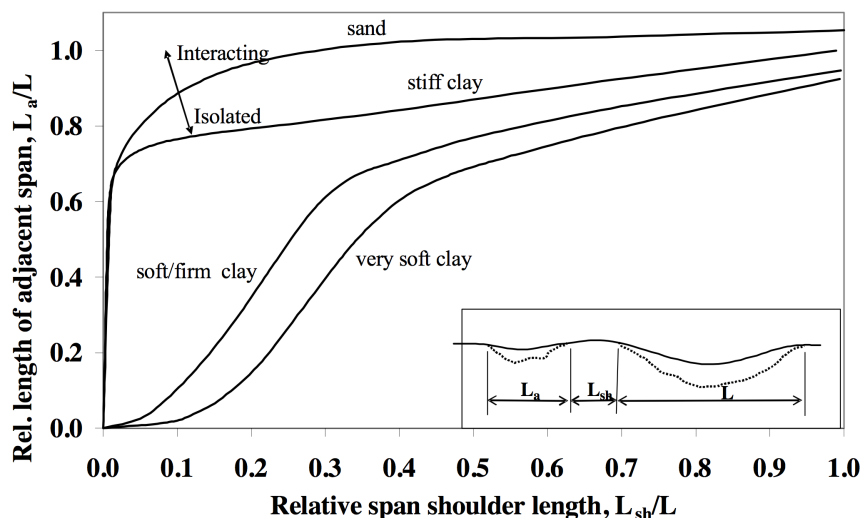
Figure 2.10: Indicative classification of free spans according to DNV-RP-F105

Table 2.1: Classification of free spans according to Statoil internal documents

Continuous	Intermittent	Clear	Multi span
$L_{sh} > 6\,m$	Minimum two spans with $L_{sh} < 6\,m$	Part of intermittent AND $L > 12\,m$	Several spans separated by $L_{sh} < 1\,TD$

not, is depending on different factors: soil properties, adjacent span. shows how the relationship between soil types, length of adjacent span, and span shoulder length according to DNV standard DNV-RP-F105, see Figure 2.10.

Statoil has an internal classification of free spans, in addition to DNV's classification. According to Statoil internal documents, they divide spans in four categories: continuous, intermittent, clear and multi-span. A continuous span has a shoulder length exceeding six meters, and a span length of any size. An intermittent span is a span area with minimum two spans having a shoulder length shorter than six meters, and of any length. Any sub span in an intermittent span with length longer than 12 meters is classified as clear, and any sub span separated by a boulder smaller than $1\,TD$ is a multi-span. Statoil's classification is summarised in Table 2.1.

Part from classifying the free spans according to interaction, a coarse classification of response behaviour is also presented in DNV-RP-F105. It is a good screening tool for further analysis and classification. The response behaviour is based on the normalised span length in Table 2.2.

Spans with normalised lengths less than 30 do not need further fatigue analysis. All spans with normalised lengths above 30 need a simplified analy-

Table 2.2: Classification of response behaviour according to DNV-RP-F105

Range	Response description
$L/D < 30$	**Very little dynamic amplification.** Normally not required to perform comprehensive fatigue design check. Insignificant dynamic response from environmental loads expected and unlikely to experience VIV.
$30 < L/D < 100$	**Response dominated by beam behaviour.** Typical span length for operating conditions. Natural frequencies sensitive to boundary conditions (and effective axial force).
$100 < L/D < 200$	**Response dominated by combined beam and cable behaviour.** Relevant for free spans at uneven seabed in temporary conditions. Natural frequencies sensitive to boundary conditions, effective axial force (including initial deflection, geometric stiffness) and pipe "feed in."
$200 < L/D$	**Response dominated by cable behaviour.** Relevant for small diameter pipes in temporary conditions. Natural frequencies governed by deflected shape and effective axial force.

Table 2.3: Classification of flow regime

Range	Flow regime
$\beta < 0.5$	Wave dominant - waves superimposed by current
$0.5 < \beta < 0.8$	Wave dominant - current superimposed by waves
$0.8 < \beta$	Current dominant

sis: Fat Free if a span is isolated or FEA if spans are interacting or experience multi-mode behaviour.

2.3.3   Classification of Flow Regime

This project will conform to DNV-RP-F105 that provide a simplified method for determining whether current or waves are dominant. The flow regimes are classified based on the current flow velocity ratio:

$$\beta = \frac{U_c}{U_c + U_w} \tag{2.38}$$

where U_c is current velocity, U_w is wave velocity; both at pipeline level. The current flow velocity ratio is used to determine the flow regime from Table 2.3. For this study β exceeds 0.8.

Chapter 3

Methodology

This project is a parameter study of boulder supports, more specifically boulder location and contact length. The methodology chosen for this study is to investigate different multi-span configurations representing a situation with intermediate boulder supports, by using a conventional free span assessment methodology. A numerical analysis of the static configuration and dynamic behaviour of a free spanning pipeline in ANSYS® is conducted, followed by a semi-empirical analysis of pipeline free span fatigue lifetime in FatFree. Validation of the numerical analysis will be a qualitative method based on face validity by domain experts.

This chapter explains the analysis process used to perform the parameter study, with a detailed description of each step with important considerations.

3.1 The Analysis Process

Static solution

The first step in the analysis process is to establish the static configuration of the span by applying pipeline and content weight (incl. coating, in an operational state). ANSYS 12.0 is used to complete this step. Input data are listed in section 3.2. The static solution provides input for the dynamic analysis in the next step.

Dynamic solution

Preceding the static solution is the modal analysis of the span. ANSYS 12.0 is used for this task as well. The natural frequencies with corresponding modes and mode shapes are identified, and stress amplitudes are calculated. These are to be used further in the fatigue life analysis in FatFree.

Fatigue life analysis

A fatigue life analysis is conducted in FatFree 10.6 for all span cases in section 3.2.3. Input data are provided in sections 3.2.1 and 3.2.2. It is crucial to remember that direct mode shape for the full multi-span section have to be input - not the response data for each span consecutively, this gives a completely wrong (non-conservative) fatigue life. The output from the fatigue life analysis is von Mises stresses for a ultimate limit state (ULS) check and fatigue life in both IL and CF direction.

3.2 Study Design

This chapter contains all information and input data used in the study for pipeline, soil and the different cases that have been investigated.

3.2.1 Pipeline

Table 3.1: Pipeline data

PARAMETER	MAGNITUDE	UNIT
TD	1.196 (47)	$m\,(inch)$
OD	1.084 (42)	$m\,(inch)$
ID	1.016 (40)	$m\,(inch)$
t_s	0.034 ($1^1/3$)	$m\,(inch)$
t_c	0.050 (2)	$m\,(inch)$
t_{corr}	0.006 ($^1/4$)	$m\,(inch)$
σ_Y	448	MPa
σ_T	531	MPa
E	207	GPa
ν	0.3	
α	1.17×10^{-5}	$^{\circ}C^{-1}$
ρ_s	7850	kg/m^3
ρ_c	3040	kg/m^3
ρ_{corr}	900	kg/m^3
ρ_{cont}	1500	kg/m^3
k_c	0.25	
f_{cn}	42	MPa

3.2.2 Soil

Table 3.2: Soil properties

PARAMETER	MAGNITUDE	UNIT
Soil type	*Clay − hard*	
K_V	32	*MPa*
K_L	23	*MPa*
$K_{V,S}$	3.4	*MPa*
Soil type	*Rock − boulder*	
K_V	66	*MPa*
K_L	45	*MPa*
$K_{V,S}$	4	*MPa*

3.2.3 Cases

Table 3.3: The different span cases investigated

CASE	CASE #	SPAN CHARACTERISTICS
Case 1 (1:2)	1-1	Single span length $100\,m$
	1-2	Multi-span length $100\,m$, boulder $0.5\,m$, span ratio 2
	1-3	Multi-span length $100\,m$, boulder $1\,m$, span ratio 2
	1-4	Multi-span length $100\,m$, boulder $2\,m$, span ratio 2
	1-5	Multi-span length $100\,m$, boulder $4\,m$, span ratio 2
	1-6	Multi-span length $100\,m$, boulder $6\,m$, span ratio 2
	1-7	Multi-span length $100\,m$, boulder $8\,m$, span ratio 2
	2-1	Multi-span length $100\,m$, boulder $0.5\,m$, span ratio 1
	2-2	Multi-span length $100\,m$, boulder $1\,m$, span ratio 1
	2-3	Multi-span length $100\,m$, boulder $2\,m$, span ratio 1
	2-4	Multi-span length $100\,m$, boulder $4\,m$, span ratio 1
	2-5	Multi-span length $100\,m$, boulder $6\,m$, span ratio 1
	2-6	Multi-span length $100\,m$, boulder $8\,m$, span ratio 1
Case 3	3-1	Multi-span length $100\,m$, boulder moved along x-axis from $x = 0$ to $x = 50$ in increments of $5\,m$

3.3 Numerical Analysis

For this study ANSYS 12.0 is chosen as the numerical analysis tool. This is a finite elemental method tool that will be used to calculate eigenfrequencies and -modes. Consecutively, these results will be used to calculate fatigue lifetime and maximum dynamic and static stress on the pipeline. For this study the non-linear analysis package is used. The model used is illustrated in Figure 3.1.
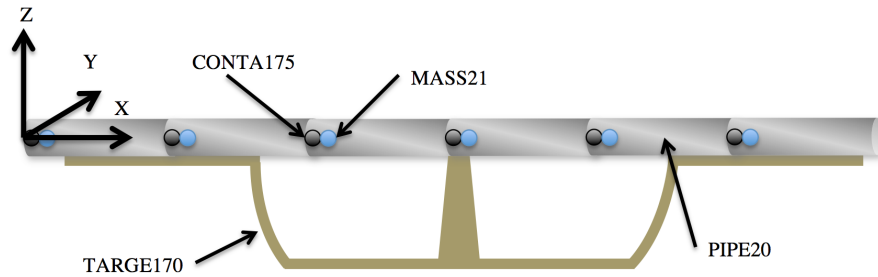
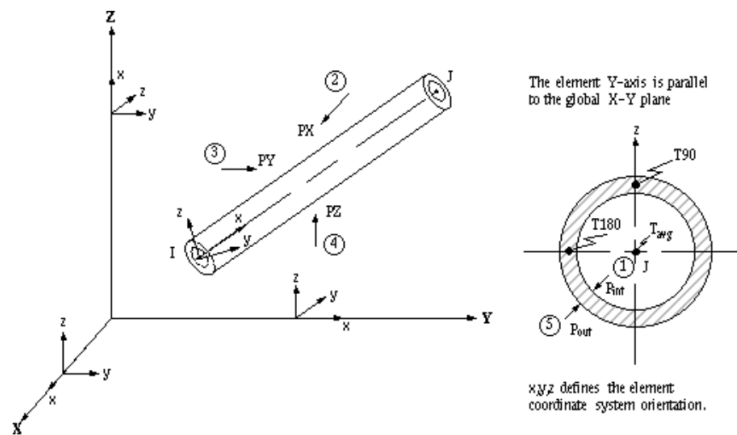**Figure 3.1:** Finite element model of free span section of pipeline

Figure 3.2: PIPE20 finite element [2]

3.3.1 ANSYS Finite Elements

The finite element types chosen for this study are the following:

Pipeline Finite Element

The finite element chosen to represent the pipeline is the elasto-plastic pipe element PIPE20. PIPE20 was chosen because the study is concerned with a 3D problem with translational movement in all three dimensions, as well as rotation around all three axes. One also wanted to include possible plastic effects resulting from high bending moments.

PIPE20 is represented in a Cartesian coordinate system and with six degrees of freedom at each element node (u_x, u_y, u_z, θ_x, θ_y, θ_z). Internal and external pressure is applied as a distributed surface load. The coordinate system and degrees of freedom for PIPE20 are illustrated in Figure 3.2
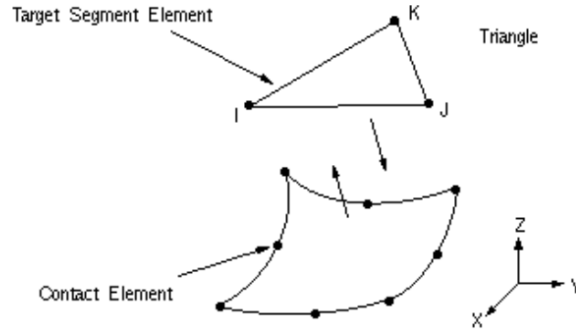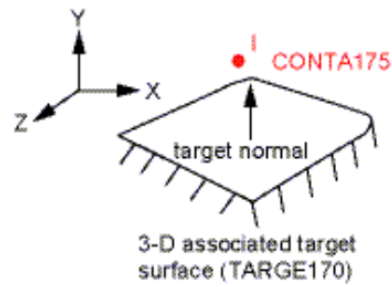
Figure 3.3: TARGE170 finite element [1]

Figure 3.4: CONTA175 finite element [4]

Seabed Finite Element

The seabed is modelled by a rigid target surface element TARGE170. The seabed is a 3D surface, hence, the reason for not choosing the 2D rigid surface element TARGE169. TARGE170 has three degrees of freedom (u_x, u_y, u_z) as can be seen in Figure 3.3. TARGE170 is coupled with a contact element (CONTA175 in this study) by a shared set of real constants.

Contact Element

The 3D nodal to surface contact element CONTA175 is used to model the contact and sliding between the seabed and pipeline. This element is coupled to the seabed element TARGE170. Several models of friction are allowed: Coulomb friction, shear stress friction and a user defined friction model. An illustration of the contact element is shown in Figure 3.4.
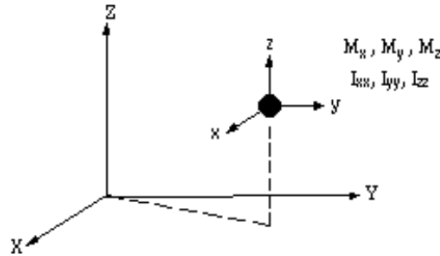
Figure 3.5: MASS21 finite element [3]

Structural Mass Element

To model added mass due to the pipeline being submerged in water the point element MASS21 is used. This is a point mass having the possibility for six degrees of freedom (u_x, u_y, u_z, θ_x, θ_y, θ_z), a concentrated mass in each coordinate direction and rotary inertias around each coordinate axis. The element is illustrated in Figure 3.5.

3.3.2 Boundary Conditions

Of great importance for fatigue lifetime of a free span are end conditions, here referred to as start and end of a free span, and model length, referred to as the total length of pipeline modelled.

End Conditions

There are three end conditions specified in DNV-RP-F105: fixed-fixed, pinned-pinned and sand seabed. Free body diagrams of the three support conditions are shown in Figure 3.6, Figure 3.7 and Figure 3.8 on page 34.

These end conditions will result in different natural periods, T_n of a specific free span. The pinned-pinned support condition will refer to a rocky seabed, rock dumping supporting a significant part of the pipe circumference, or other artificial supports. For a pinned-pinned condition T_n will be long governed by the pipeline section's natural period, vibration amplitudes larger and a higher likelihood of interaction with neighbouring spans than for a fixed-fixed condition. In a model this end condition is modelled as a spring with very high stiffness (almost infinitely).

Fixed-fixed support conditions refers to a free span with buried ends, rock covered ends, concrete slab constrained ends or other artificial means of clamping. A fixed-fixed end condition will give shorter T_n because of the constraints on movement and the amplitudes are smaller than for a pinned-pinned situation. Also, interaction with neighbouring spans seems very unlikely as ends are fixed for movement. To represent this in a model

Table 3.4: Comparison of different end conditions

SUPPORT CONDITION	FATIGUE LIFE
RP-F105	195
Fixed-fixed	149000
Pinned-pinned	0.98
Fixed-pinned	3290
Span length $96\,m$, TD $1.192\,m$	

the ends need to be completely fixed, and there is no interaction between soil and pipe.

In between these two extremities is the third case with sandy seabed. For a sandy seabed a pipeline will sink into it, governed by the stiffness of the sand, and in a model, interactions between seabed and pipeline is modelled as a spring with a specific stiffness representing stiffness of a sandy seabed or by the target surface method used in this study.

One can conclude from the natural period and level of interaction between neighbouring spans that a pinned-pinned end condition will most likely give the highest fatigue lifetime while a fixed-fixed condition gives the lowest. This is also indicated by a small comparison study shown in Table 3.4.

Model Length

According to DNV-RP-F105 the boundary conditions applied at the ends of the free span section should represent the continuity of the pipeline. To incorporate this statement it is important to model sufficient length of pipeline in both ends of a free span section. Wang et al.[18] presents a method for determining sufficient model length by calculating the virtual anchor space, i.e. the distance from the free span section to the location where the pipeline is fully restrained due to friction. This virtual anchor distance can be calculated by

$$z = \frac{P_i \cdot \pi \cdot D^2}{4 \cdot F_{friction}} \cdot \left[\frac{4 \cdot t_s \cdot E \cdot \alpha \cdot \triangle T}{P_i \cdot D} + (1 - 2\nu) \right] \qquad (3.1)$$

where z is the virtual anchor distance, P_i is the internal pressure, $\triangle T$ is the temperature difference between installation temperature and operating temperature and

$$F_{friction} = \mu \cdot m_{submerged} \qquad (3.2)$$

is frictional force (Coulomb) where μ is the friction coefficient and $m_{submerged}$ is the submerged unit weight (in $^N/_m$) of the pipeline.

Wang et al. [18] states that the virtual anchor method would require a total model length of approximately $2000\,m$ for a $50\,m$ span, but comparisons of a $400\,m$ and $2000\,m$ model show a difference of only 3%. Hence, in this study a model length of $1000\,m$ is chosen for boulders larger than $2\,TD$ and $500\,m$ for boulders smaller than $2\,TD$. Another reason for not choosing a longer model length is due to convergence troubles in ANSYS.

3.3.3 Pipeline-Soil Interaction

The pipeline-soil interaction is modelled as Coulomb friction and accounted for in this model by including the dynamic soil stiffness in the global stiffness matrix of the system. Because soil damping is considered very small it is neglected in this study. Coulomb friction is a part of the CONTA175 finite element that is modelled at each node.

3.4 Calculation of Fatigue Lifetime

Calculation of fatigue lifetime is done in FatFree 10.6, according to DNV-RP-F105, either with a semi-empirical method or by input from modal analysis by means of FEA.

FatFree is a spreadsheet tool developed by Det Norske Veritas as a simple but powerful analysing tool to assess fatigue life for free spans. The software is developed based on DNV-RP-F105 Free spanning pipelines, which is one of DNV's many recommended practices and offshore standards for the oil and gas industry.

FatFree is a spreadsheet-based software where the user inputs boundary conditions, pipeline data, environmental data and modal data. The environmental data used in FatFree are either return period values, scatter diagrams, histograms, or Weibull distribution for waves and currents. These data are obtained from met ocean reports.

One has two choices for analysis in FatFree, either single or multiple mode. A single mode analysis is for screening purpose only. Multi-mode analysis is conducted if a FEA has been conducted, which is especially relevant if a free span is very long and experience cable behaviour (ref. Table 2.2)

If a span is not interacting with other spans according to the classifications made in Figure 2.10 or Table 2.1 one performs a single span analysis, either single or multi-mode.

If a span is interacting with neighbouring spans one needs to perform a multi-span analysis. As input data a modal analysis is conducted by means of FEA to identify mode amplitudes and corresponding natural frequencies. Natural frequencies and mode shapes are directly used in FatFree. In FatFree one has the option to either use response data for a single span multi-mode

analysis or direct mode shape input for a multi-span multi-mode analysis; hence the latter is used in this study.

Figure 3.6: Pinned-pinned support (rocky seabed)

Figure 3.7: Fixed-fixed support (concrete anchors or rock cover)

Figure 3.8: Sand seabed

Chapter 4

Results

This chapter is a summary of all results obtained in the analysis. There were two specific parameters this study set out to investigate (ref. section 1.4): boulder location and boulder-pipeline contact length. The results for these two parameters are presented in section 4.1 and 4.2 respectively. A discussion of these results is presented in chapter 5.

4.1 Boulder Location

Boulder location was analysed in case 3 by varying the location of one boulder approximately equal to one TD along the x-axis of the pipeline free span section.

From Figure 4.1 one can see that a boulder located far to the left results in very low fatigue lifetimes; even lower than without a boulder. And the most critical location is at a relative distance (x/L) of 0.15.

From Figure 4.3 it is evident that case 2 – boulders located at the modal null-point of the second mode – is more suppressive at lower normalised contact lengths than case 1. Moreover, Figure 4.1 indicates that boulders located closer to either end of the free span section is far more critical for fatigue life than boulders located at modal null-points; contrary to what was expected beforehand.

In addition, referring to Figure A.8, A.9 and A.10 one can see that for these cases cross flow induced in-line vibrations is present, shifting the order of IL and CF modes.

4.2 Contact Length

The analyses done in case 1 and 2 with different contact lengths indicate as expected, that for increasing contact length at modal null-points (mode 3 and 2 respectively) the pipeline free span section's fatigue lifetime increases. Moreover, very small boulders located at modal null-points have a low but

Table 4.1: f_n for the first three modes of the multi-spans

CASE	Cont. length	$f_{n,IL,1}$	$f_{n,IL,2}$	$f_{n,CF,1}$
1-1	$0\,m$	0.25	0.69	0.34
1-2	$0.5\,m$	0.60 (140%)	1.51 (119%)	0.62 (82%)
1-3	$1.5\,m$	0.62 (3%)	1.58 (5%)	0.63 (2%)
1-4	$2\,m$	0.60 (−3%)	1.57 (−1%)	0.62 (−2%)
1-5	$4\,m$	0.62 (3%)	1.67 (6%)	0.64 (3%)
1-6	$6\,m$	0.63 (2%)	1.72 (3%)	0.65 (2%)
1-7	$8\,m$	0.63 (0%)	1.71 (−1%)	0.65 (0%)

significant suppressive effect on VIV. This can be seen from Figure 4.2, where fatigue lifetime is close to a situation without boulders for a $0.5 - 1\,TD$ boulder. After normalised contact lengths of 1.5 fatigue lifetime increases dramatically and the suppressive effect of boulders are prominent, even when located at modal null-points.

From Table 4.1 one can also see that even though the contact length is very small ($< 1\,TD$) the natural frequencies are increased drastically, and remains fairly constant for increasing contact lengths, which, is in-line with what discussed in the preceding paragraph.

It can also be seen from Figure 4.2 and the results from case 1 that when the normalised contact length exceeds 4 fatigue lifetime is dramatically increased.
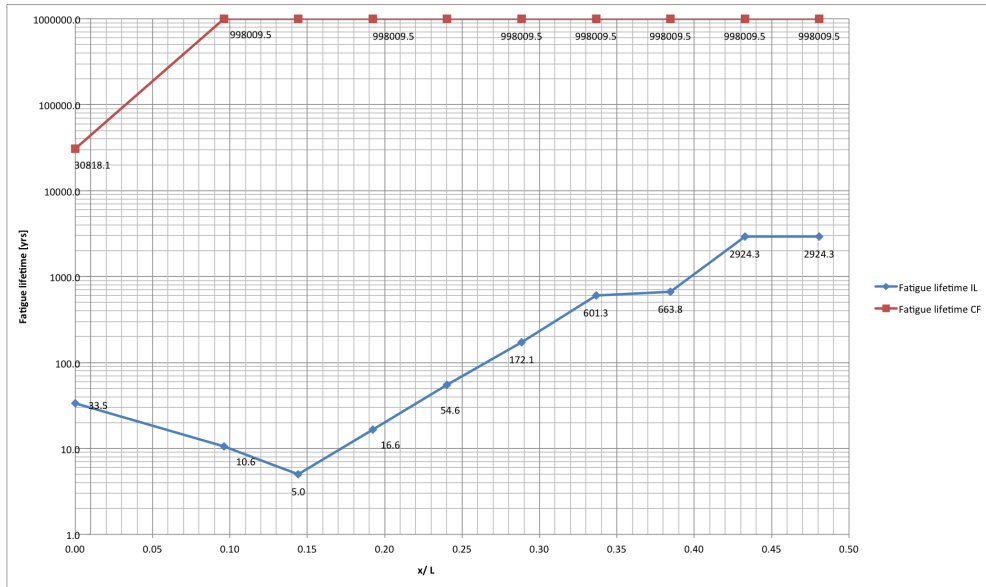
Figure 4.1: Fatigue lifetime versus normalised boulder location along pipeline axis (x-axis). Contact length $= 1\,TD$, multi-span length $= 100\,m$
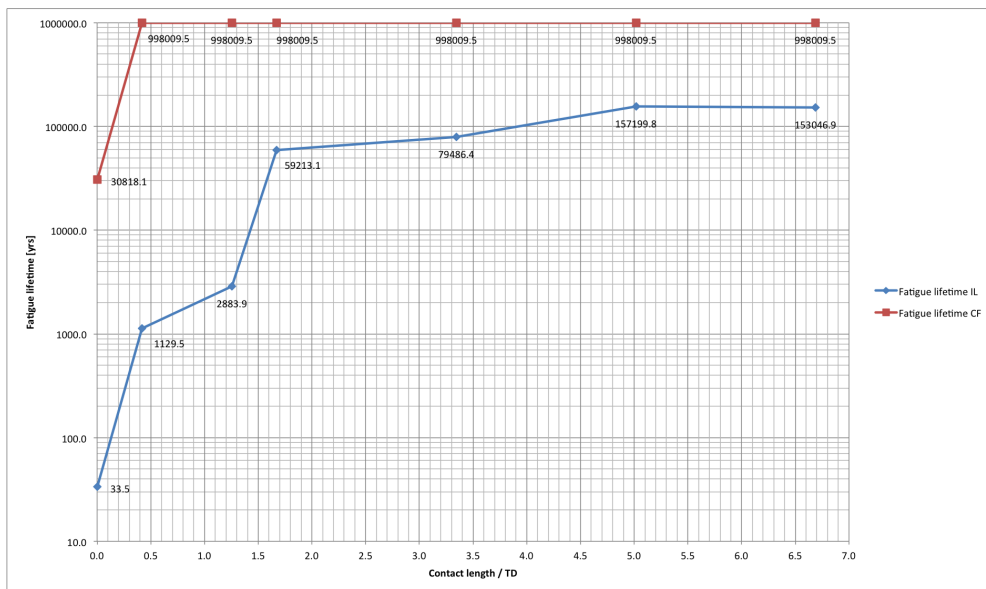
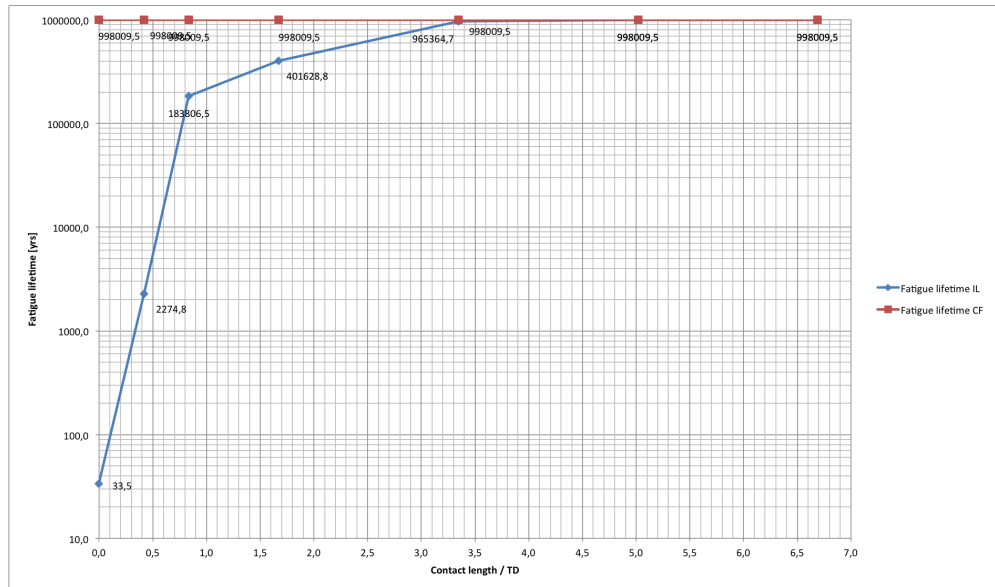**Figure 4.2:** Fatigue lifetime versus normalised contact length from case 1. Span ratio $= 2 : 1$, multi-span length $= 100\,m$

Figure 4.3: Fatigue lifetime versus normalised contact length from case 2. Span ratio $= 1 : 1$, multi-span length $= 100\,m$

Chapter 5

Discussion

The results in Figure 4.1 was not as expected, as the hypothesis was that boulders at modal locations would resemble a situation equal to a single span with equal length. But the results say that the most critical location, even more critical than a single span situation, is at a relative position 0.15 along the x-axis. This can be explained by the combination of natural frequency and stress amplitude at this location being the most critical. This point is also further explained further down in the text, because these two factors combined are important for fatigue lifetime as indicated by the results.

By comparing Figure 4.2 and 4.3 a conclusion could be that a boulder located at the modal null-point of the third mode results in a lower fatigue lifetime, hence, being a more critical situation than a boulder located at the modal null-point of the second mode. This is because case 1 yields a lower natural frequency than case 2, and is more prone to VIV at current velocities relevant for large pipelines outside the Norwegian coast. However, both cases remove the first mode completely, which is the most dangerous one, thus resulting in a drastic increase in fatigue lifetime by introducing a boulder at these locations.

When considering rock dumping or artificial supports as VIV suppression methods it looks from the results above that the optimal location of a boulder is at the midpoint, giving the most beneficial natural frequency relative to VIV.

From Figure 4.2 and 4.3 it is seen that after the normalised contact length exceeds 1.5 fatigue lifetime increases drastically, and beyond 4 is extremely large. This can be explained by the fact that the two neighbouring spans are not interacting to a great extent, and interaction diminishes as contact length increase. Moreover, because L/D is below 60 for both individual spans in both multi span cases (see Table 5.1) , span behaviour is beam dominant; hence, multi-mode vibrations are less likely.

A further explanation of the fatigue life results for different contact lengths should be seen in the light of Figure 5.1, 5.2, 5.3, 5.4, 5.5 and

5.6, which represent stress amplitudes, natural frequencies and maximum vibration amplitudes for the different contact length cases.

By analysing and comparing these figures one see that until a certain threshold the fatigue lifetime is governed by increasing stress amplitudes, which increase for increasing contact lengths and increasing distance along the x-axis of the pipeline. One can also see that the vibration amplitudes are larger for contact lengths $<1\,TD$ than for an equivalent single span if one of the multi spans that are considerably longer than the other, i.e. for case 1 (span ratio 2:1) this effect is evident but for case 2 (span ratio 1:1) this effect is almost non-existing. For case 1 the fatigue lifetimes remain relatively low because of the increasing stress amplitude for case 1 until the contact length increase beyond $1\,TD$. For case 2 this effect is not as evident and fatigue lifetimes increase substantially only by introducing a boulder.

After contact lengths increase beyond $1\,TD$ the natural frequency of the multi span will increase beyond the VIV region and fatigue lifetime increases drastically accordingly. Again this effect is more evident for case 1 than case 2, and the reason for this is that when one of the multi-span sections remain relatively large compared to the neighbouring span the natural frequency remains low enough for VIV, even for larger contact lengths.

In a comparison with Statoil and DNV's classification of free spans (see Table 5.2) only the cases with $<1\,TD$ contact length is regarded as interacting multi spans. From the results presented in the previous chapter contact lengths up to $4\,m$ can be regarded as interacting, although not causing very low fatigue lifetimes. Both Statoil and DNV's classifications are reasonable according to the results, where Statoil's multi-span category should signal that further investigation into multi-span interaction should be conducted.

In the aftermath of this study it is evident that a more suitable choice of environmental data and span characteristics should have been chosen, such that cross flow vibrations also contributes. The environmental data used in this study, which is representative for a real world situation, are seen unable to produce cross-flow vibrations of the modelled spans. For this reason, the graph in Figure 4.2 show a nearly constant – very high – fatigue lifetime for CF vibrations. Only in-line vibrations are activated for these environmental data, which is also seen from the example calculation in equation 2.32 and 2.33.

In addition, the investigated pipeline characteristics were inspired by a large-dimension pipeline on large water depth. Consequently, the free span risk is somewhat reduced by this fact, and this situation was not as suitable as first expected for this study.

One important experience made during the analysis work was the calculation of multi-span multi-mode fatigue, as this was not as straight forward as first expected. Further research should look at how multi-spans could efficiently be assessed in a rigorous way. The method chosen in this study is conservative, because it assumes that different modes do not influence each

Table 5.1: L/D ratio

CASE	L/D
1 single span	84
1 small span	28
1 long span	56
2 individual span	42
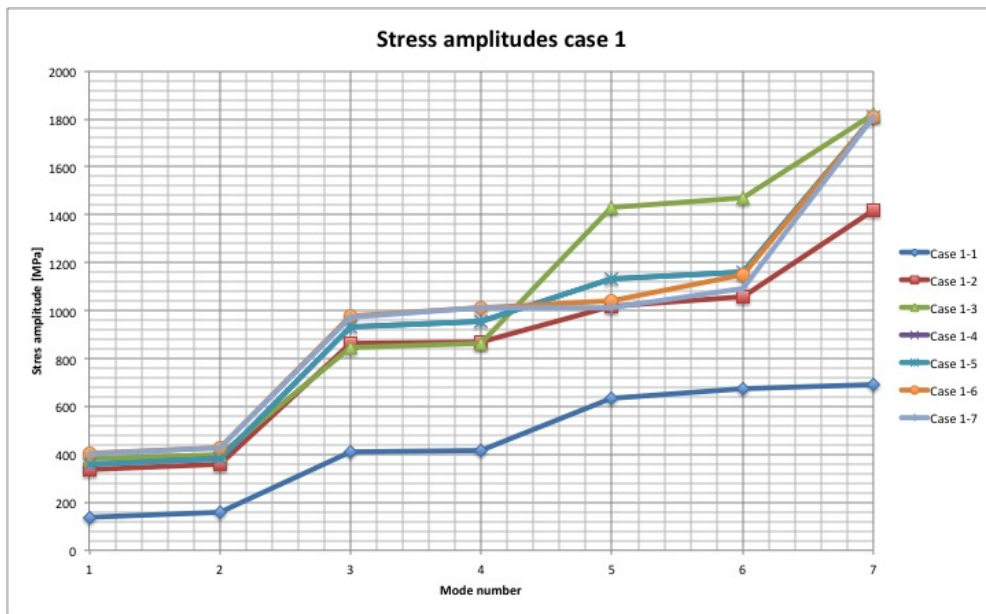
Figure 5.1: Stress amplitudes for case 1

other, i.e. all amplitudes are assumed to be fully active when the corresponding mode is active. Consequently, this study should be considered as a first-order analysis indicating the influential magnitude each of the two parameters have on fatigue lifetime.
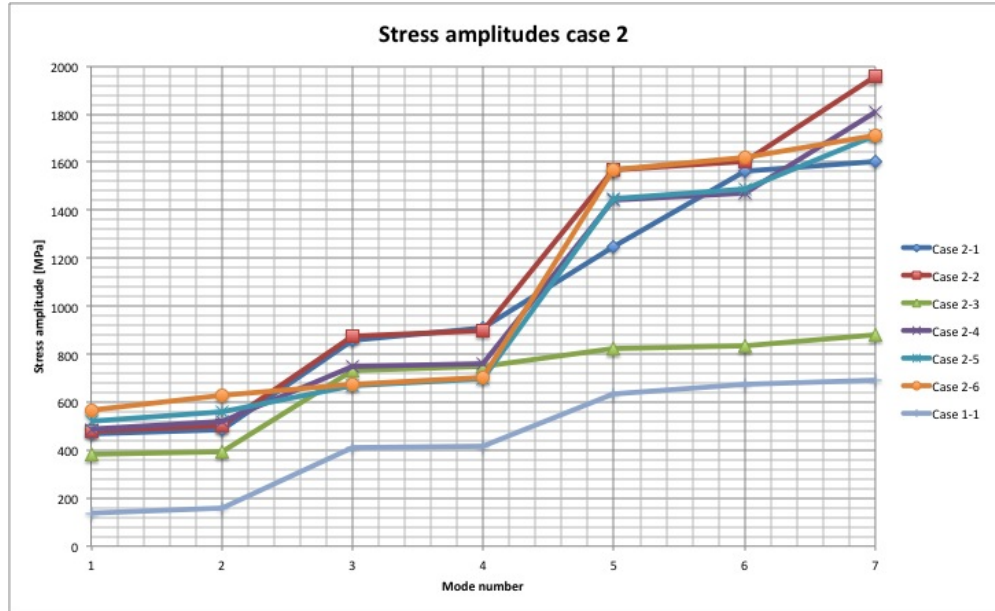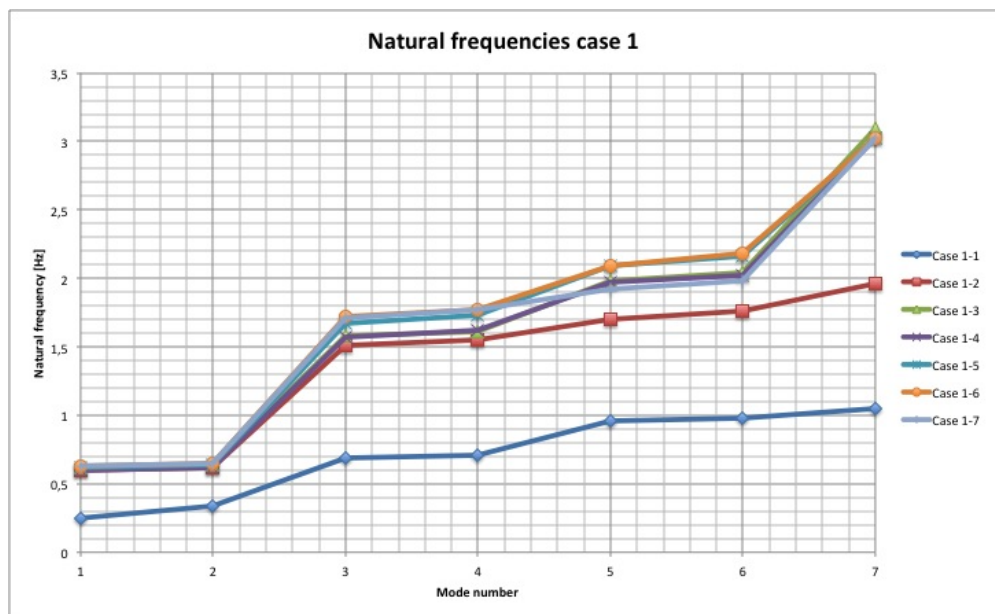
Figure 5.2: Stress amplitudes for case 2

Figure 5.3: Natural frequencies for case 1
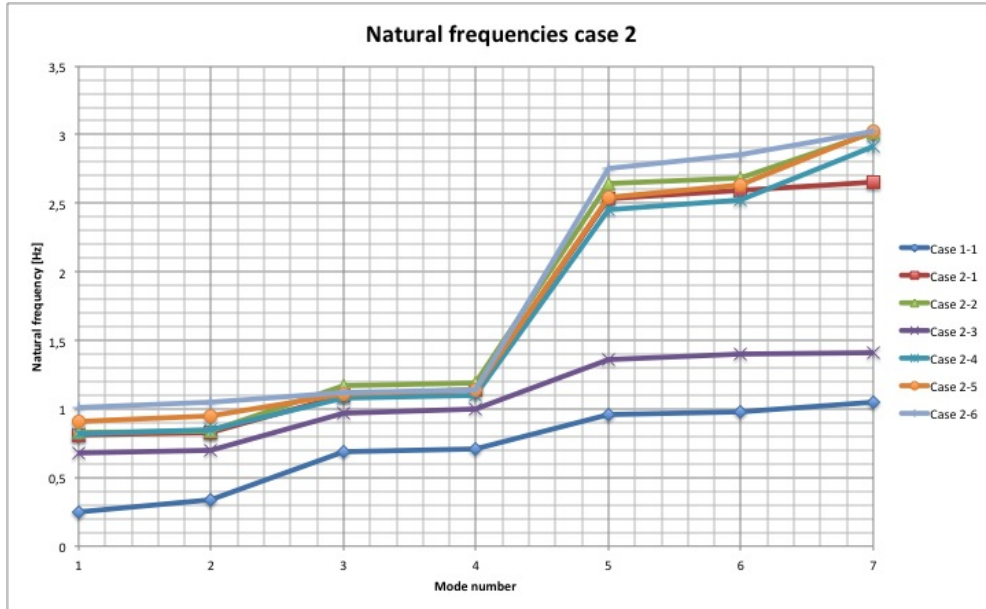
Figure 5.4: Natural frequencies for case 2
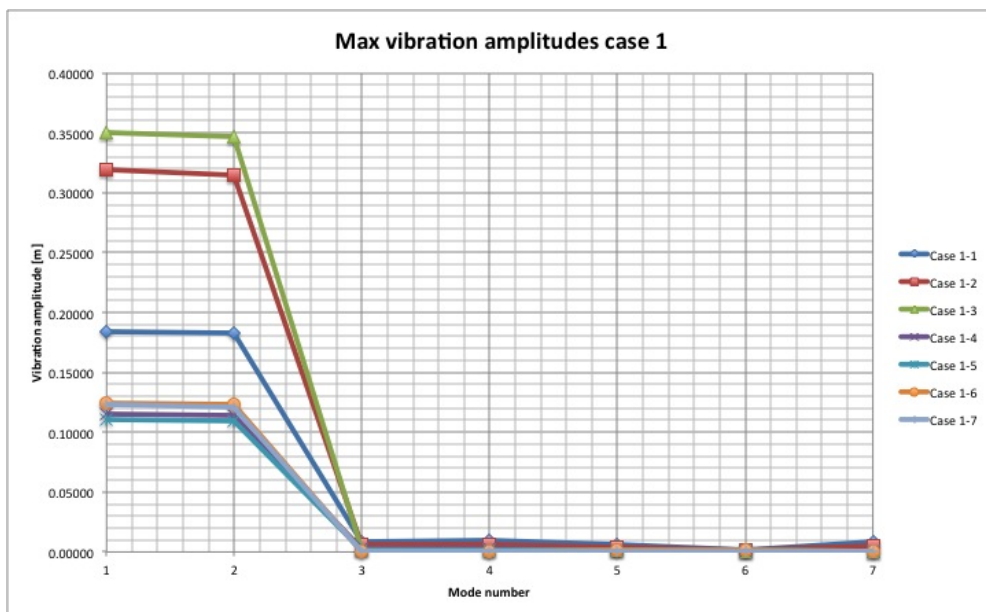
Figure 5.5: Maximum vibration amplitudes for case 1
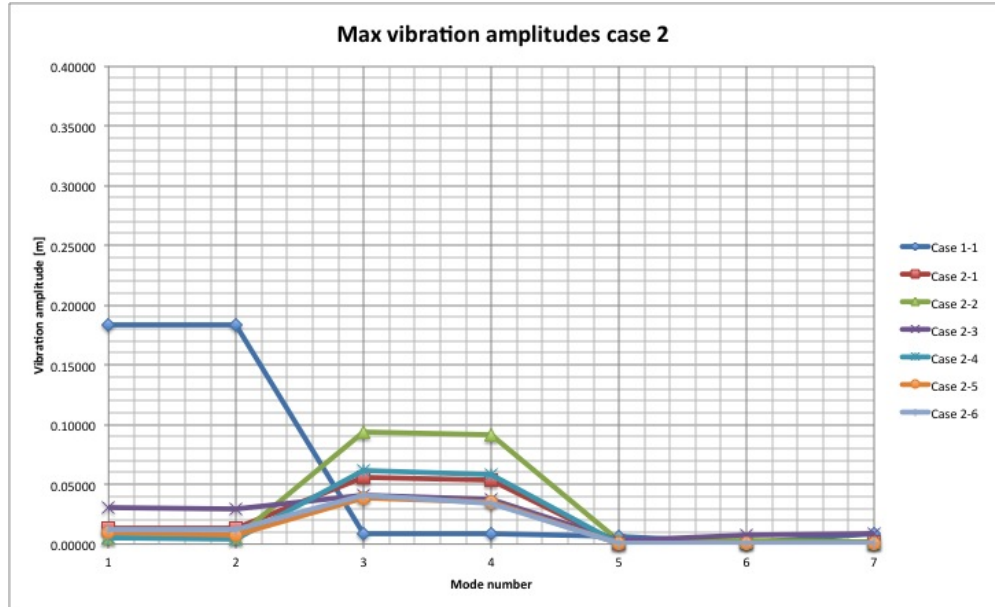
Figure 5.6: Maximum vibration amplitudes for case 2

Table 5.2: Case 1 and 2 in relation to Statoil and DNV classification

CASE	STATOIL	DNV
1-1	N/A	N/A
1-2	Multi span	Interacting
1-3 – 1.5	Intermittent, clear	Isolated
1.6 – 1.7	Continuous	Isolated
2.1 – 2.2	Multi span	Interacting
2.3 – 2.4	Intermittent, clear	Isolated
2.5 – 2.6	Continuous	Isolated

Chapter 6

Conclusions

Returning to the research questions put forward in section 1.4 to be answered by this study:

1. Is a multi span with boulders located at vibrational null-points equivalent to a single span with a length equal to all multi spans combined?

2. How will contact length of boulders influence the dynamic behaviour of a multi span?

Question 1 was investigated in section 4.1 and the conclusion is that locating boulders at modal null-points will have a suppressive effect on VIV and increase fatigue lifetime of the pipeline free span section. In other words, a multi-span with boulders at modal null-points are not equal to an equivalent single span, much because the critical first mode is removed.

Secondly, boulders located at the modal null-point of the second mode is more suppressive than boulders located at the modal null-point of the third mode. The author believes for a span ratio of 2:1 the larger span will, because it is longer than the spans in a 1:1 span ratio-case, cause the second in-line mode of the multi span to vibrate at a lower natural frequency; and consequently closer to the shedding frequency.

Question 2 was investigated in section 4.2 with the following conclusions. First, a low contact length will cause neighbouring spans to influence each others vibrations, i.e. a multi span situation.

Second, even low contacts ($<1\,TD$) will have a suppressive effect on the dynamic behaviour of a multi span. In other words, a small boulder present in a free span section will have a suppressive effect, thus increase the fatigue life of this pipeline section, compared to a situation without boulders.

A third conclusion from this study is that when considering span correction by introducing supports, these supports should be located as close to the midpoint as possible. Due to the fact that this configuration results in the most beneficial dynamic behaviour of the pipeline; moving the natural frequency farthest away from the VIV range.

Chapter 7

Further Work

The free spans considered in this study are not very long, and for all the multi spans the expected dynamic behaviour is mainly beam dominated, hence, multi-mode behaviour is not expected. Multi-span section with longer individual spans should be investigated to look how cable dominated behaviour (i.e. multi-mode) influence the fatigue lifetime for different boulder configurations.

Another interesting area of further research is to investigate the influence of a pipeline not resting permanently on a boulder during VIV. By reason this situation will cause the concrete to crack on this location possibly leading to higher stress concentration factors and lower pipeline strength. This is not considered in this study, as the pipeline is assumed to be stationary on top of the boulder.

The last suggestion for further work, which was also mentioned earlier, is to develop a rigouros and practical method of multi-span fatigue life assessment. The current practice is difficult and tedious to perform. A faster and more efficient method would make it easier to include effects of neighbouring spans and the different effects on mode shape, vibration amplitude and maximum stress amplitudes.

Bibliography

[1] ANSYS. 4.170 TARGE170 3-d target segment (UP19980821). http://mostreal.sk/html/elem_55/chapter4/ES4-170.htm.

[2] ANSYS. 4.20 PIPE20 plastic straight pipe (UP19980821). http://www.ansys.stuba.sk/html/elem_55/chapter4/ES4-20.htm.

[3] ANSYS. 4.21 MASS21 structural mass (UP19980821). http://www.ansys.stuba.sk/html/elem_55/chapter4/ES4-21.htm.

[4] ANSYS. CONTA175. http://www.sharcnet.ca/Software/Fluent13/help/ans_elem/Hlp_E_CONTA175.html.

[5] Arthur P. Boresi and Richard J. Schmidt. *Advanced Mechanics of Materials*. Wiley, 6 edition, October 2002.

[6] William D. Callister. *Materials Science and Engineering: An Introduction*. Wiley, 7 edition, February 2006.

[7] E. Finnemore and Joseph Franzini. *Fluid Mechanics With Engineering Applications*. McGraw-Hill Science/Engineering/Math, 10 edition, October 2001.

[8] Olav Fyrileiv and Leif Collberg. Influence of pressure in pipeline design - effective axial force. Halkidiki, Greece, June 2005.

[9] J.M.J. Journée and W.W. Massie. Lecture notes in offshore hydromechanics 1st ed, 2001.

[10] J.R. Morison, J.W. Johnson, and S.A. Schaaf. The force exerted by surface waves on piles. *Journal of Petroleum Technology*, 2(5), May 1950.

[11] E.G. Paterson. Approximate solutions of the navier-stokes equations, 2005.

[12] Singiresu S. Rao. *Machanical Vibrations*. Pearson Education India, 2003.

[13] Günter Schewe. On the force fluctuations acting on a circular cylinder in crossflow from subcritical up to transcritical reynolds numbers. *Journal of Fluid Mechanics*, 133:265–285, 1983.

[14] Håvar Sollum and Knut Vedeld. A semi-analytical model for free vibrations of free spanning offshore pipelines. Research Report in Mechanics 02, University of Oslo, December 2012.

[15] Tore Søreide, Gunnar Paulsen, and Finn Gunnar Nielsen. Parameter study of long free spans. In *The proceedings of the eleventh (2001) international offshore and polar engineering conference.*, Stavanger, Norway, June 2001. ISOPE.

[16] B. Mutlu Sumer and Jorgen Fredsoe. *Hydrodynamics Around Cyclindrical Structures*. World Scientific Pub Co Inc, revised edition, September 2006.

[17] Det Norske Veritas. DNV-RP-F105 free spanning pipelines, February 2006.

[18] James Wang, F. Steven Wang, Gang Duan, and Paul Jukes. VIV analysis of pipelines under complex span conditions.pdf. Harbin, China, January 2009. The Deepwater Offshore Science Society.

[19] C. H. K. Williamson. The existence of two stages in the transition to three-dimensionality of a cylinder wake. *Physics of Fluids (00319171)*, 31(11):3165, November 1988.

Appendix A

Mode Charts
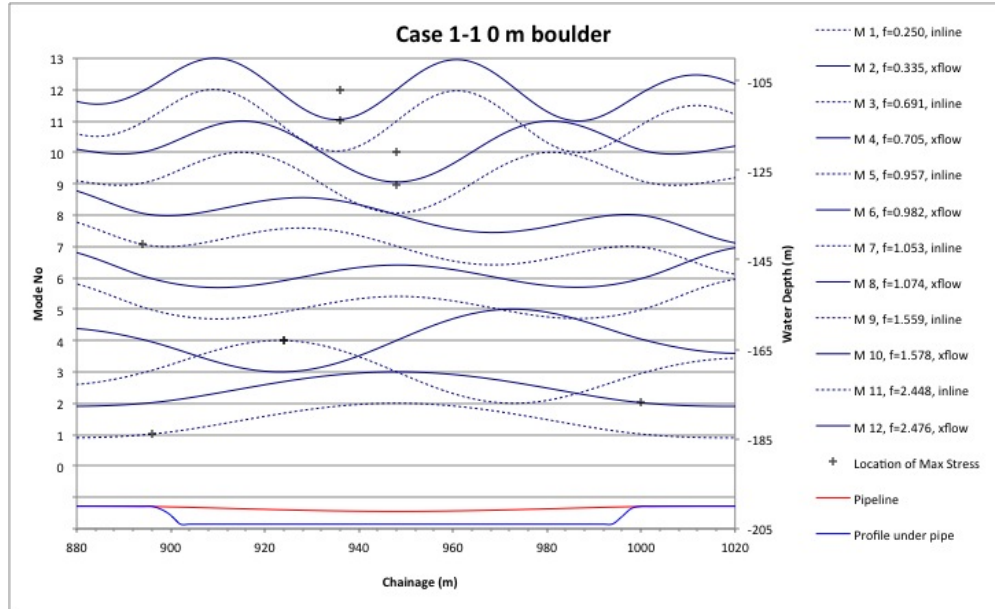
Figure A.1: Vibration modes and natural frequencies for case 1-1
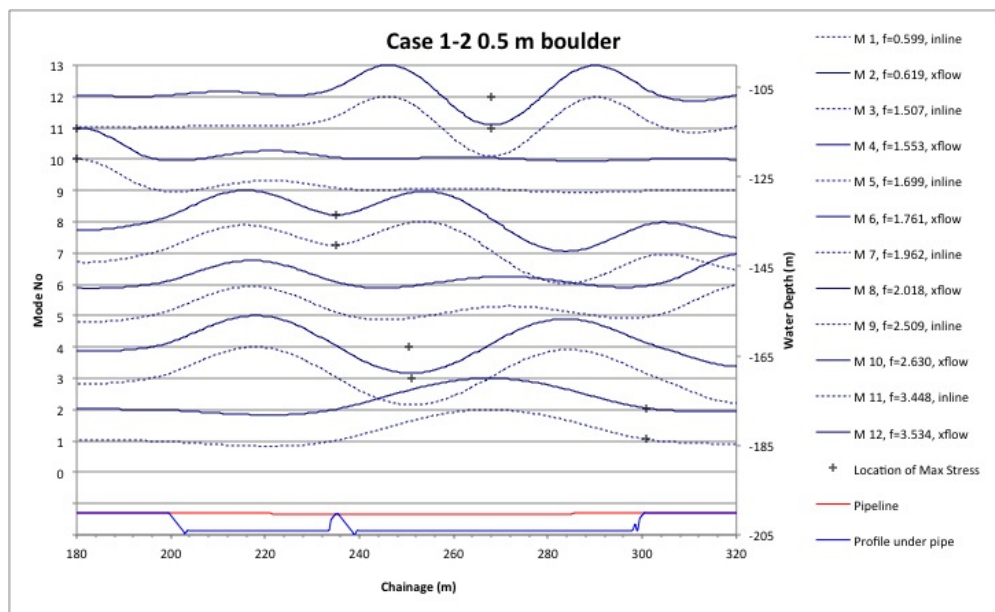
Figure A.2: Vibration modes and natural frequencies for case 1-2
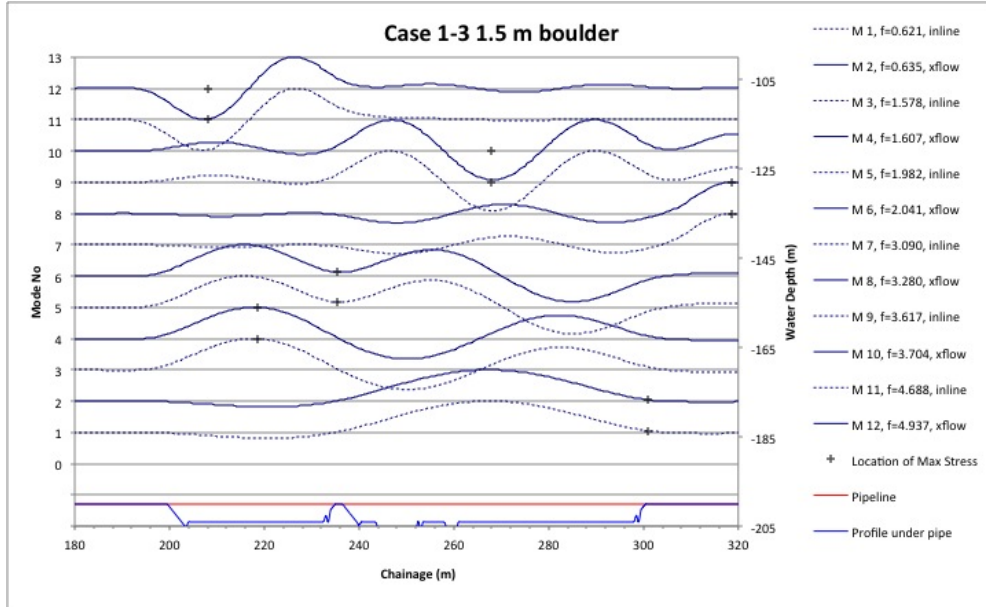
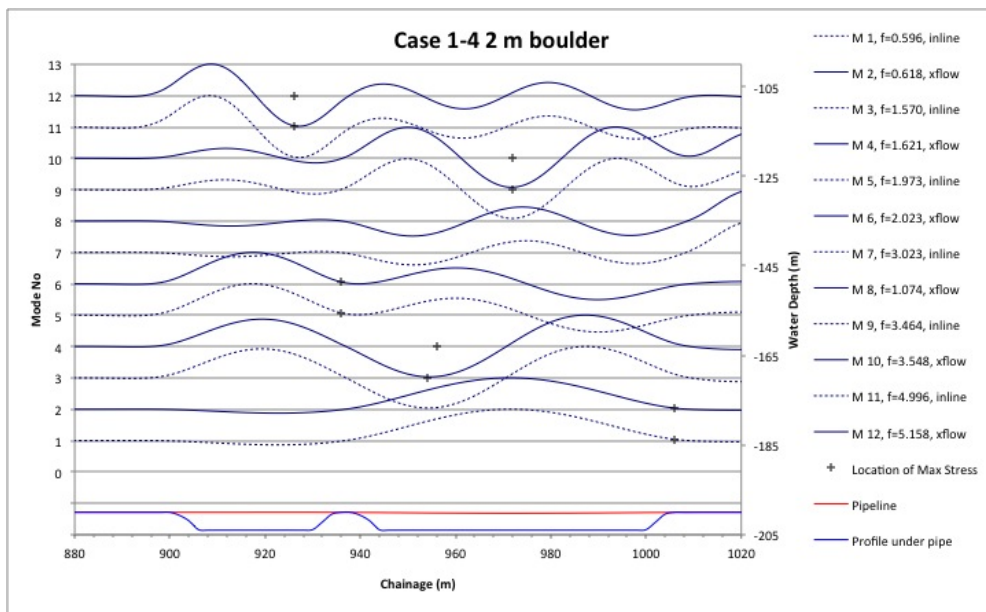**Figure A.3:** Vibration modes and natural frequencies for case 1-3

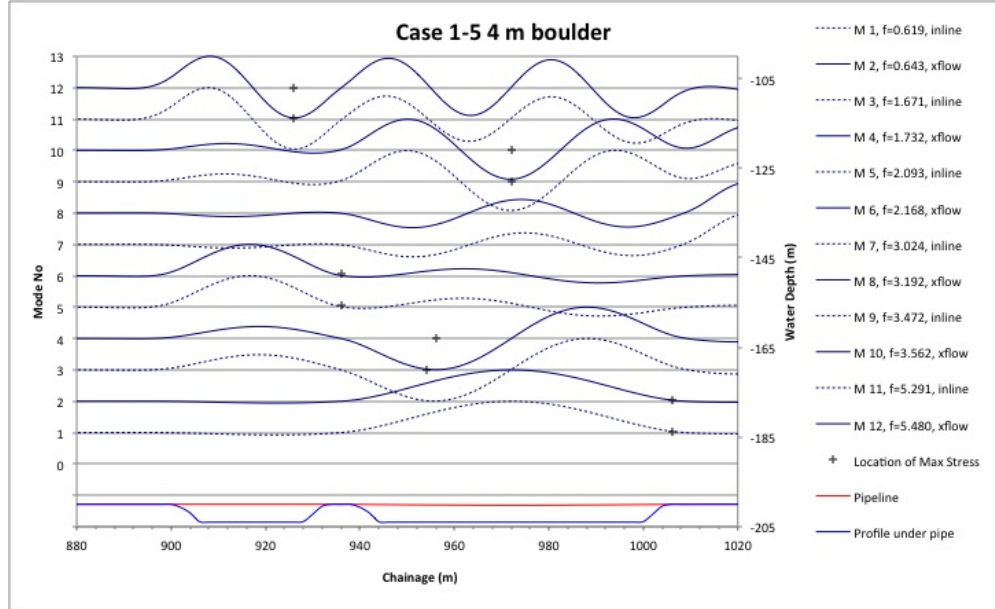**Figure A.4:** Vibration modes and natural frequencies for case 1-4

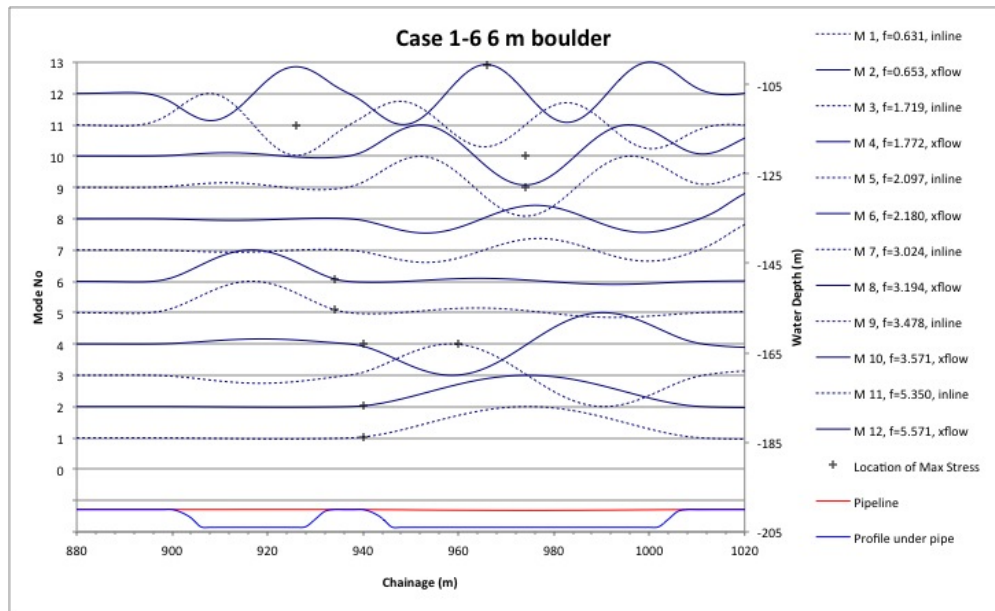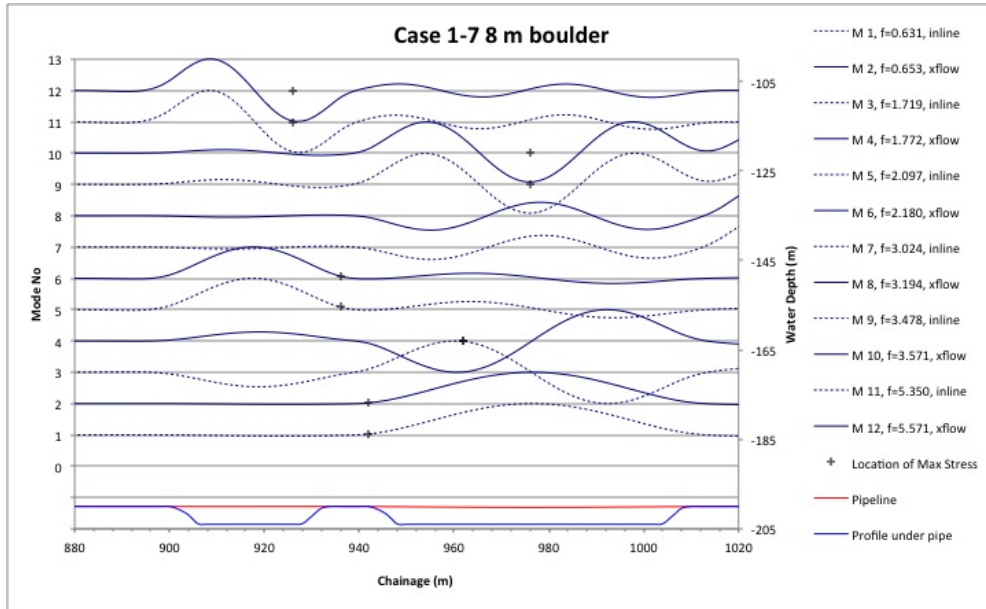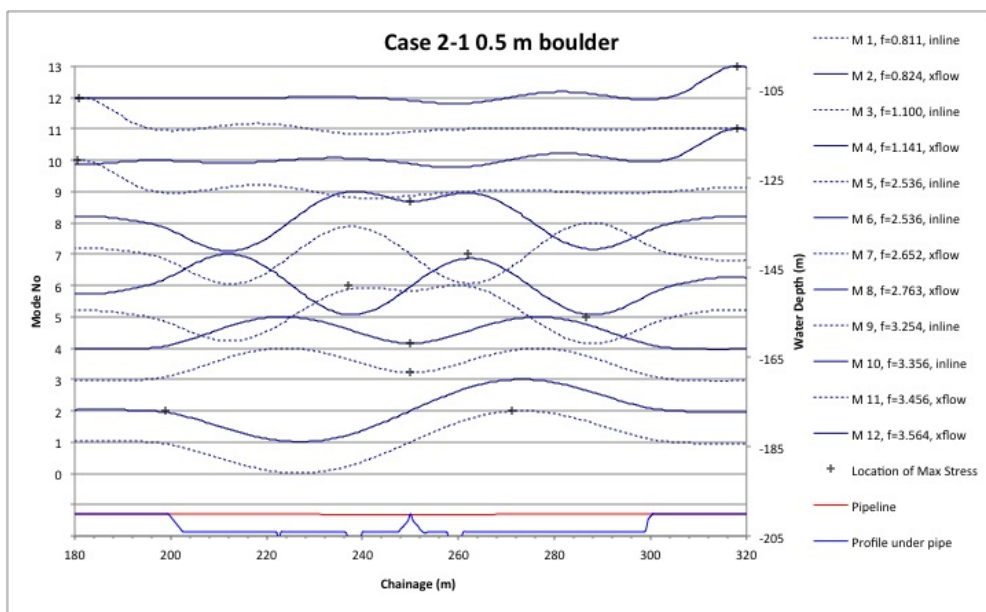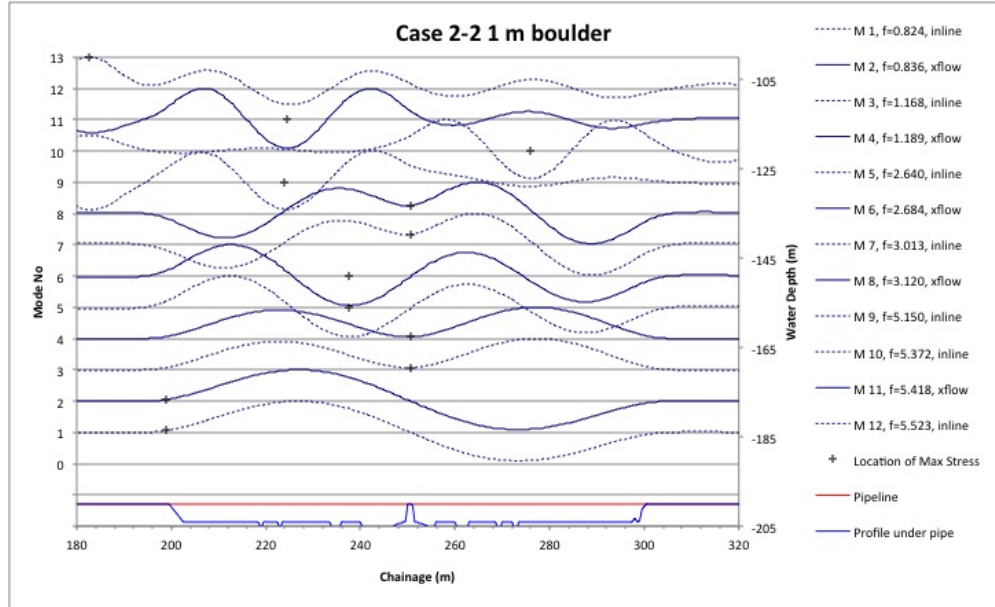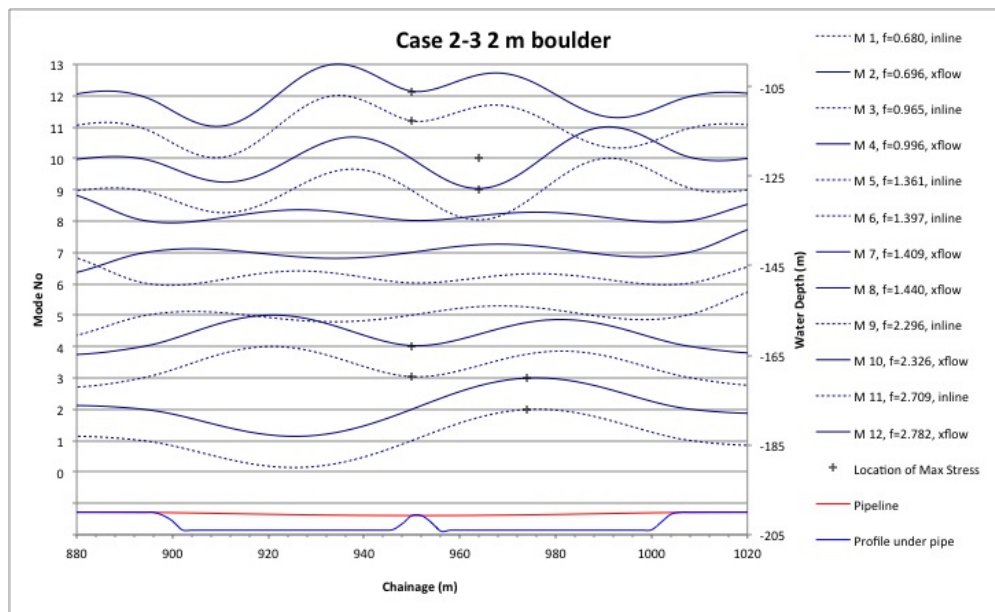**Figure A.5:** Vibration modes and natural frequencies for case 1-5

Figure A.6: Vibration modes and natural frequencies for case 1-6

Figure A.7: Vibration modes and natural frequencies for case 1-7

Figure A.8: Vibration modes and natural frequencies for case 2-1

Figure A.9: Vibration modes and natural frequencies for case 2-2

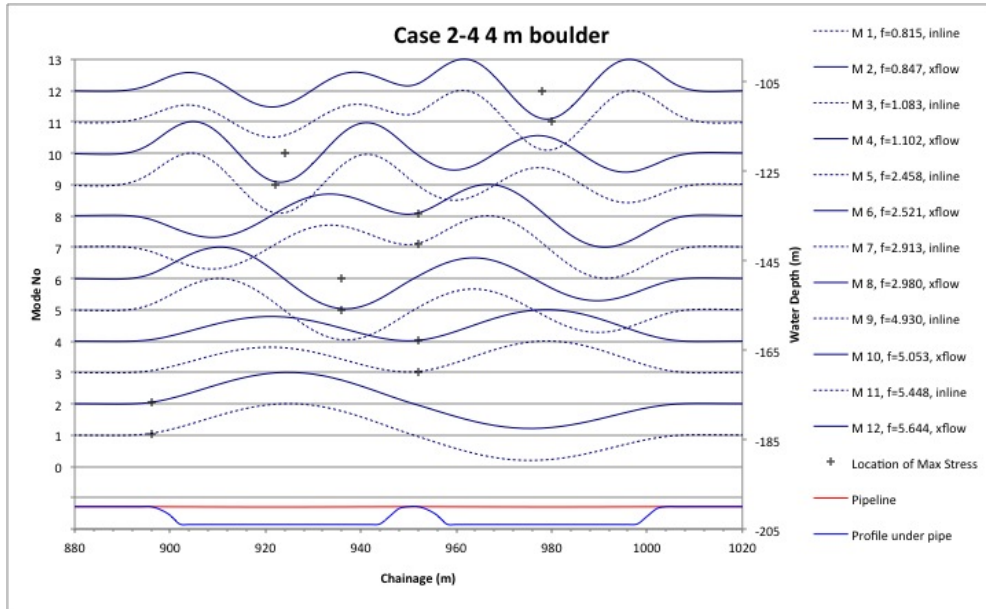**Figure A.10:** Vibration modes and natural frequencies for case 2-3

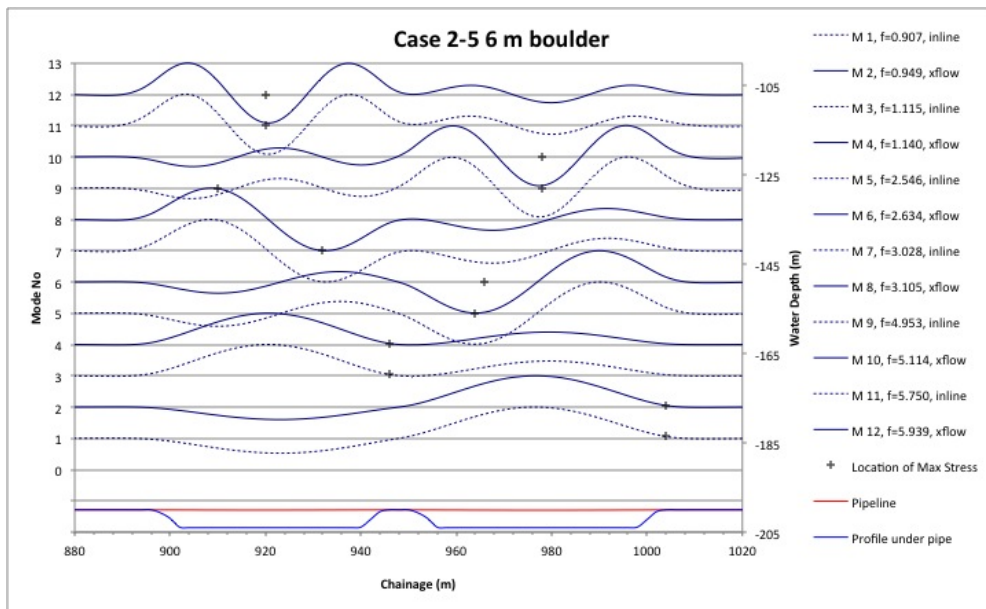**Figure A.11:** Vibration modes and natural frequencies for case 2-4

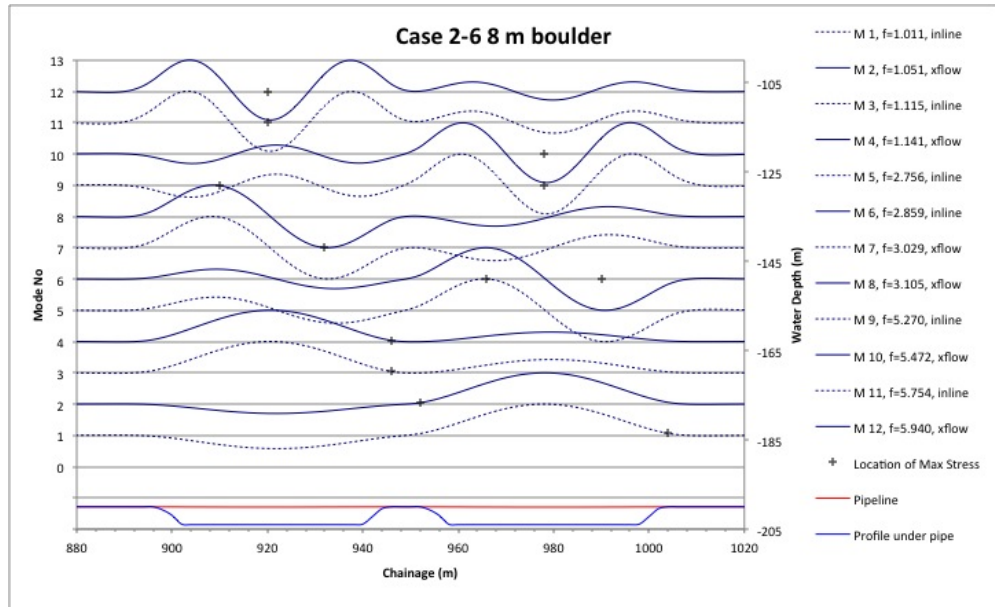**Figure A.12:** Vibration modes and natural frequencies for case 2-5

Figure A.13: Vibration modes and natural frequencies for case 2-6